ENVIRONMENTAL RADIOLOGY OF NORTHERN PART OF ZAMFARA STATE, NIGERIA

BY

CHRISTOPHER MMADUABUCHI ODOH

DEPARTMENT OF PHYSICS

AHMADU BELLO UNIVERSITY,

ZARIA, NIGERIA

OCTOBER, 2018

ENVIRONMENTAL RADIOLOGY OF NORTHERN PART OF ZAMFARA STATE, NIGERIA

BY

Christopher Mmaduabuchi ODOH, B.Sc. (UNN) 2011

MSc/Nuclear Physics/P15SCPY8012

A DISSERTATION SUBMITTED TO THE SCHOOL OF POSTGRADUATE STUDIES,
AHMADU BELLO UNIVERSITY, ZARIA
IN PARTIAL FULFILLMENT OF THE REQUIREMENTS FOR THE AWARD
OF MASTER OF SCIENCE IN NUCLEAR PHYSICS

DEPARTMENT OF PHYSICS,
FACULTY OF PHYSICAL SCIENCES,
AHMADU BELLO UNIVERSITY,
ZARIA, NIGERIA

OCTOBER, 2018

DECLARATION

I declare that the work in this Dissertation entitled Environmental Radiology of Northern Part of Zamfara State, Nigeria has been carried out by me in the Department of Physics, Ahmadu Bello University. The information derived from the literature has been duly acknowledged in the text and a list of references provided. No part of this thesis was previously presented for another degree or diploma at this or any other institution.

Christopher MmaduabuchiOdoh	.....	.....
Name of Student	Signature	Date

CERTIFICATION

This Dissertation entitled 'ENVIRONMENTAL RADIOLOGY OF NORTHERN PART OF ZAMFARA STATE, NIGERIA' by CHRISTOPHER MMADUABUCHI ODOH (M.Sc. P15SCPY8012) meets the regulations governing the award of the degree of Master of Science (Nuclear Physics) of the Ahmadu Bello University, and is approved for its contribution to knowledge and literary presentation.

Dr. N. N. Garba	.....	.....
(Chairman of Supervisory Committee)	Signature	Date
Prof. RabiuNasiru	.....	.....
(Member, Supervisory Committee)	Signature	Date
Prof. RabiuNasiru	.....	.....
(Head of Department)	Signature	Date
Prof. S. Z. Abubakar	.....	.....
(Dean, School of Postgraduate Studies)	Signature	Date

DEDICATION

I dedicate this Dissertation to my parents, Mr and Mrs Odoh Wilfred, whom their encouragement and support made this work a reality.

ACKNOWLEDGEMENT

I am absolutely grateful to my ebullient supervisors, Dr. N. N. Garba and Prof. RabiuNasiru for their fatherly advice, contribution, corrections, and efforts to this work.

I am also grateful to my lecturers who have contributed in one way or the other to success of this study.

I equally recognize the effort of my parents, who's their encouragements and support, have helped to the progress of this work.

ABSTRACT

This study is undertaken to measure the variation of terrestrial gamma radiation and the activity concentrations of U-238, Th-232 and K-40 in soil of Northern part of Zamfara State (Nigeria), and assess the potential health hazards associated with the exposures to the natural radiation in the area with respect to geological formations. Inspector Alert^{TM} Nuclear Radiation Monitor and HPGe gamma ray spectrometer were used for TGRD and laboratory analyses respectively. The measured TGRD rates ranged from 20.00 to 61.43 nGy/h, with mean value of 31.99 nGy/h. The mean (range) activity concentrations of U-238, Th-232 and K-40 in the soil samples were 19.43 ± 2.23 (8.82 ± 0.95 to 44.22 ± 5.78) Bq/kg, 23.26 ± 8.43 (11.02 ± 1.03 to 43.96 ± 2.15) Bq/kg and 268.62 ± 39.03 (57.45 ± 2.88 to 527.36 ± 12.38) Bq/kg respectively. These results were compared with the world average values for specific activities (i.e. 33, 45 and 420 Bq/kg) for U-238, Th-232 and K-40 respectively, and were found to be less than the worldwide average. The highest TGRD rate and activity concentrations of U-238, Th-232 and K-40 were recorded in an area underlain by Older Granite formation, which are enriched with high contents of radioactive materials. The radiological hazards to the public in the studied area was assessed by estimating mean values of radium equivalent activity, external hazard index, and activity utilization index for the soil samples were found to be 71.674± 7.099 Bq/kg, 0.1936± 0.0192, and 0.4688± 0.0448 respectively.In addition, the mean values of absorbed gamma dose rates, annual outdoors effective dose rates, and excess lifetime cancer risk for both TGRD rate measurements and spectrometric analyses were found to be 31.99 nGy/h, 0.0393 mSv/y and 137.6×10^{-6}, and 33.467 ± 3.367 nGy/h, 0.0412 ± 0.0040 mSv/y and $(144.0 \pm 14.0) \times 10^{-6}$ respectively.

TABLE OF CONTENTS

Title	Page
Cover page	i
Title Page	iii
Declaration	iv
Certification	v
Dedication	vi
Acknowledgement	vii
Abstract	viii
Table of Contents	ix
List of Tables	xii
List of Figures	xiii
List of Appendices	xiv
List of Abbreviations	xv
List of Symbols	xvii
CHAPTER ONE	1
INTRODUCTION	1
1.1 Background of the study	1
1.2 Statement of the Problem	2
1.3 Justification of the study	3
1.4 Aim and Objectives	3
1.5 Scope of the study	4
CHAPTER TWO	5
LITERATURE REVIEW	5
2.1 Radioactivity	5
2.2 Environmental Radioactivity	5
2.2.1 Natural Radioactivity	6
2.2.1.1 Primordial radionuclides	6
2.2.1.2 Cosmogenic radionuclides	9

2.2.2 Artificial Radioactivity 10

2.3 Detectors 10

2.3.1 High purity germanium (HPGe) detector 10

2.3.2 Operations of HPGe detectors 11

2.3.3 Energy resolution and efficiency of HPGe 12

2.4 Review of Previous Works 12

CHAPTER THREE 17

METHODLOLGY 17

3.1 Materials 17

3.2 Study Area 18

3.2.1 Geology of the study Area 18

3.3 Terrestrial Gamma Radiation Dose Rate Measurements 19

3.3.1 Calibration of the Inspector Alert Meter 20

3.3.2 Measuring with the Inspector Alert Meter 20

3.4 Radiological mapping 21

3.5 Soil Sample Collection 22

3.6 Sample Preparation 22

3.7 Experimental Set-up 23

3.8 Sample Analysis 24

3.9 Activity Concentration 24

3.10 Radiological Hazards 25

3.10.1 Radium equivalent activity (R_{eq}) 25

3.10.2 External hazard index (H_{ex}) 26

3.10.3 Activity utilization index (AUI) 26

3.10.4 Absorbed gamma dose rate (D_R) 26

3.10.5 Annual effective dose rate (H_R) 27

3.10.6 Excess lifetime cancer risk (ELCR) 27

CHAPTER FOUR 29

RESULTS AND DISCUSSIONS 29

4.1 Measurement of TGRD Rates 29

4.2 Radiological Mapping 33

4.3 Activity Concentrations of U-238, Th-232 and K-40 in the soil samples 35

4.4 Radiological Hazards 38

4.4.1 Radium equivalent activity 38

4.4.2 External hazard index 40

4.4.3 Activity utilization index 42

4.4.4 Absorbed gamma dose rate 44

4.4.5 Annual outdoor effective dose rate 46

4.4.6 Excess lifetime cancer risk 48

CHAPTER FIVE 51

SUMMARY, CONCLUSIONS AND RECOMMENDATIONS 51

5.1 Summary 51

5.2 Conclusions 51

5.3 Recommendations 53

REFERENCES 54

APENDICES 58

LIST OF TABLES

List of Tables **Page**

Table 3.1: Successions of geological formations and their rock types 19

Table 3.2: Sample labels of each geological formation 22

Table 4.1: Mean TGRD rates for each of the seven L.G.As of the studied area 31

Table 4.2: Mean TGRD rates for each the geological formation 32

Table 4.3: Comparison of mean TGRD rates of Northern Zamfara with other Countries and the world 32

Table 4.4: Calculated activity concentrations of U-238, Th-232 and K-40 in the soil 36

Table 4.5: Comparison of activity concentrations in soil of Northern part of Zamfara with other countries and the world 37

Table 4.6: Radium Equivalent Activity 39

Table 4.7: External Hazard Index 41

Table 4.8: Activity Utilization Index 43

Table 4.9: Absorbed Gamma Dose Rate 45

Table 4.10: Annual Outdoor Effective Dose Rate 47

Table 4.11: Excess Lifetime Cancer Risk 49

LIST OF FIGURES

List of Figures **Page**

Figure 2.1: Decay Series of U-238, U-235 and Th-232 8

Figure 2.2: Decay Chain of K-40 9

Figure 2.4: Block diagram of HPGe detector setup 11

Figure 3.1: Digitized geological map of the study area 18

Figure 3.2: Location points of gamma dose rate measurements 22

Figure 4.1: A Radiological map of the studied area 34

Figure 4.2: Activity concentrations of U-238, Th-232 and K-40 for each sample 38

Figure 4.3: Radium Equivalent Activity for each sample 40

Figure 4.4: External hazard index for each sample 42

Figure 4.5: Activity Utilization index for each sample 44

Figure 4.6: Absorbed Gamma dose rate for each sample 46

Figure 4.7: Annual Outdoor Effective dose rate for each sample 48

Figure 4.8: Excess Lifetime Cancer Risk for each sample 50

LIST OF APPENDICES

List of Appendices	Page
Appendix I: Measured TGRD rates with the coordinates	58
Appendix II: Plates	65

LIST OF ABBREVIATIONS

NORMs - Naturally Occuring Radioactive Materials

TGRD - Terrestrial Gamma Radiation Dose

NaI(Tl) - Sodium Iodide doped with Thallium

HPGe – High Purity Germanium

SI – International System of Units

UNSCEAR – United Nations Scientific Committee on the Effects of Atomic Radiation.

WNA – World Nuclear Association

BDL – Below Detection Limit

PM – Photomultiplier

MCA – Multi-Channel Analyzer

FWHM – full width at half maximum

CARMS – Compact Aerial Radiation Monitor System

GT – Gamma Tracer

GIS – Geographical Information System

U.S.A. – United States of America

N.G.S.A. – Nigerian Geological Surveying Agency

CPM – counts per minute

CPS – counts per second

ID – Identity

NIRPR – National Institute of Radiation Protection and Research

ICRP – International Commission on Radiological Protection

et al. – other people are also involved

ELCR – Excess Lifetime Cancer Risk

AUI – Activity Utilization Index

Std - Standard

Devi - Deviation

LIST OF SYMBOLS

Co-60	–	Cobalt-60
Cs-137	–	Cesium-137
K-40	-	Potassium-40
Th-232	–	Thorium-232
U-238	–	Uranium-238
U-235	–	Uranium-235
Ca-40	–	Calcium-40
Ar-40	–	Argon-40
Pb-206	–	Lead-206
Pb-207	–	Lead-207
Pb-208	–	Lead -208
Pb-214	–	Lead -214
K-39	–	Potassium-39
K-41	–	Potassium -41
Ra-226	–	Radium-226
Am-241	–	Americium-241
Ba-133	–	Barium-133
Na-22	–	Sodium-22
Eu-155	–	Europium-155
Sb-125	–	Antimony-125
Mn-54	–	Manganese-54
Zn-65	–	Zinc-65
Bi-214	–	Bismuth-214
Ac-228	–	Actinium-228

Tl-208	–	Thallium-208
H_{ex}	–	External hazard index
D_R	–	Absorbed Gamma Dose Rate
H_R	–	Annual Outdoor Effective Dose Rate
Ra_{eq}	–	Radium Equivalent Activity
nGy/h	–	nano-Gray per hour
mSv/y	–	milli-Sievert per year
Bq/kg	–	Becquerel per kilogram
MeV	–	mega-electron volts
keV	–	kilo-electron volts
mR/h	–	milli-Roentgen per hour
μSv/h	–	micro-Sievert per hour
cm	–	centimetre
Bq	–	Becquerel
g	-	gram
s	–	second
Ci	–	Curie
$\boldsymbol{\beta}$	–	Beta
eV	–	electron volt

CHAPTER ONE

INTRODUCTION

1.1 Background of the Study

Environment is naturally radioactive, irrespective of the locations on the Earth's crust (Garba*et al.*, 2016). This has been so since the creation of the Earth (Innocent *et al.*; 2014). The radioactive substances are continuously emitting ionizing radiation that affects living organisms due to continuous exposure from the ground, building materials, air, and from human body (Osimobi*et al.*, 2015; Garba*et al.*, 2016). These ionizing radiations from the natural sources are the major sources of human exposure to radiations, which arise mainly from cosmic rays and from terrestrial radionuclides that are occurring at trace levels in all soil formations (Tzortzis*et al.*, 2002). These do not include other sources of exposure from medical sources and nuclear reactor breakdown or accident (Faanu*et al.*, 2012; Garba*et al.*, 2016). The level of exposure to the terrestrial radionuclides in the soils of any region of the Earth depend mainly on the geological and geographical land formations (Girigisu*et al.*, 2013; Garba*et al.*, 2016), and human activities in the region, such as mining, making and using fertilizers, oil and gas production (WNA, 2016).

Naturally Occurring Radioactive Materials (NORM) include all the radioactive elements found in the environment and exist in different geological features such as rocks, soils, vegetations, water and air (Innocent *et al.*; 2014). The two main sources of NORMs are terrestrial and cosmic radiations. The terrestrial radionuclides consist of all the natural radioisotopes coming from the Earth's crust and mantle. They result from the primordial radionuclides such as K-40, U-238, and Th-232 decay series. These series have been in existence since the creation of the Earth and occur at trace levels in all ground formations

(Garba*et al.*, 2016). The cosmic radiation on the other hand, formed as a result of cosmic rays interaction with certain gases in the Earth's atmosphere (Osimobi*et al.*, 2015).

Human activities have enhanced the radiation level in the environment compared to the unaltered situation. For this reason, it is important to monitor the level of concentration of the terrestrial radionuclides in our environment for radiological protection as well as for the focus of setting regulatory standard (Lee *et al.*, 2009; Augustine and Aku, 2013; Innocent *et al.*, 2014, Garba*et al.*, 2016). Long lived radioactive elements such as K-40, U-238, and Th-232 and their decay products are of major concerned. The study of environmental natural radioactivity and the potential risk of exposure have been of interest to various researchers worldwide in the recent times (Aznan*et al.*, 2009; Ramali*et al.*, 2009; Girigisu*et al.*, 2012;Saleh*et al.*, 2013; Gabdo*et al.*, 2014; Innocent *et al.*, 2014; Olusegun*et al.*; 2014; Ibrahim *et al.*, 2015; Isinkaye and Emelue, 2015; Nabil *et al.*, 2015; Najib*et al.*, 2015; Osimobi*et al.*, 2015;Raghu *et al.*, 2015;Garba*et al.*, 2016).

1.2 Statement of the Problem

It is clear that radiation is part of the environment and over 85% of human exposure to radiation comes from the naturally occurring radionuclides (Garba*et al.*, 2016). Recently, World Nuclear Association reported that human activities in the environment such as mining, making and using fertilizers, oil and gas productions have the potential to increase the risk of radiation exposure to human and the environment beyond normal background levels (WNA, 2016). This result in contamination and pollution of soil and air which is an issue that need a great attention because it may cause serious health hazard, which aroused due to inhaled air from the area and consumption of foodstuff cultivated on these polluted soils. Radiation can have serious effect on the biological system through interaction with the cellular composition of the organism (Christian, 2014). The more radiation dose human receives, the greater

chance of developing cancer of various organs, haematological depression, eye cataracts, leukaemia, Erithemia, incidence of chromosome aberrations, severe nausea, loss of appetite, serious risk of infections, diarrhoea, skin peels, sterility, severe damage to central nervous system (Christian, 2014).

A thorough investigation showed that people of Zamfara State engaged in illegal gold mining as their source of income. They extract and process it themselves through unsafe and unregulated means (Udoka, 2010). It is possible the areas have been exposed to high dose of ionizing radiations. Therefore, there is need to check out the level activity concentrations of radioactive substances in the soil and air and their radiological hazard among the populace.

1.3 Justification of the Study

In Zamfara State to the best of my knowledge, there is no available data on natural radionuclide concentrations and public exposure, and has not been subjected to radiological regulatory control. Therefore, there is need to have a proper documentation of data on the radiation exposure level, which will create awareness to all the stake holders of the state, including artisanal miners, the local population, as well as the relevant regulatory authorities.

1.4 Aim and Objectives

This study aimed at assessing the environmental radiological status of Northern Zamfara State, Nigeria with respect to the geological formations.

The objectives of this study were:

I. To determine the Terrestrial Gamma Radiation Dose (TGRD) rates and produce a radiological map of the study area using ARCGIS software.

II. To determine the activity concentrations of ^{238}U, ^{234}Th and ^{40}K in soil and their radiological implications with respect to the geological formations of the study area.

III. To compare the results obtained with those of others and make recommendations for further works in the area.

IV. To further provide data/ radiological information of NorthernZamfara for future studies.

1.5 Scope of the Study

This study assesses the environmental radiological status of Northern Zamfara State, Nigeria, which covered the seven local government areas namely Bakura, Zurmi, Shinkafi, BiriniMagaji, MaradunKauraNamoda and TalafaMafara. The measurement of the TGRD rates were done using a handheld radiation survey meter and the activity concentrations of U-238,Th-232 and K-40 in the soilusing HPGe detector with respect to geological formations. A radiological map of the study area was produced using ArcGIS software version 10.3. The assessments of the radiological hazards due to the natural radiations in the study area were also carried out.

CHAPTER TWO

LITERATURE REVIEW

2.1 Radioactivity

Radioactivity also known as radioactive decay or nuclear decay, is the process by which an unstable atomic nucleus loses energy by emitting energetic particles and photons called radiations. These radiations include alpha particles, beta particles with neutrino or only neutrino in the case of electron capture, gamma ray, or electron in the case of internal conversion. A material in which its nuclei are unstable is said to be radioactive. Radioactivity is a natural phenomenon and occurs in a number of substances.

The International System of Units (SI) of radioactive activity is the becquerel (Bq), named in honour of the scientist Henri Becquerel. One Bq is defined as one transformation (or decay or disintegration) per second. The total number of radioactive atoms present in a given sample is not of much consequence; it is the disintegration rate that matters. That is why the units of radioactivity are in terms of the disintegration rate.

An older unit of radioactivity is the curie, Ci, which was originally defined as "the quantity or mass of radium emanation in equilibrium with one gram of radium (element)". Today, the curie is defined as 3.7×10^{10} disintegrations per second, so that 1 curie (Ci) = 3.7×10^{10} Bq(Evwaraye*et al.*, 2006).

2.2 Environmental Radioactivity

The environmental surroundings contain numerous radioactive materials which may be due to natural or artificial processes. Some radioisotopes, such as strontium-90 (Sr-90) and technetium-99 (Tc-99), are only produced artificially, while potassium-40 (K-40), uranium-

238, and thorium-232, are present due to natural processes, and a few isotopes, for example tritium (H-3), result from both natural and artificial processes.

2.2.1 Natural radioactivity

Natural radioactivity is the worldwide largest sources of ionizing radiation and occurs naturally as trace elements in soils, rocks and outer space. Over 85% of human absorbed radiation doses come from this source. Natural radionuclides were categorized into two according to their origin and formation: Primordial and cosmogenic (WNA, 2016).

2.2.1.1 *Primordial radionuclides*

Primordial radionuclides also known as terrestrial radionuclides consist of radioactive materials that come out of the Earth's crust and mantle. These radionuclides exit naturally in the soils and rocks and are members of uranium and thorium decay series. These chains provide terrestrial radionuclides in significance levels. Another major source of terrestrial nuclides is potassium 40 (K-40) decay chains, with long half-life (1.25 billion years) which means that it still exists in measurable quantities today.

More specifically, terrestrial radionuclides and their associated external exposure due to gamma radiation depend on the geological and geographical conditions and appear at different levels in the soils of each region in the world due to the different geological composition and content of rock from which the soil originated (UNSCEAR, 2000; Tzortzis*et al.*, 2004).

- Decay Schemes of the Primordial Nuclides:

The decay schemes of the primordial nuclides are the actinium alpha decay chains of thorium, uranium, actinium each ends with its specific lead isotope (Pb-208, Pb-206, Pb-207

respectively) and potassium-40 (K-40), which ends in either Ca-40 or Ar-40 depending on the mode of decay.

Thorium Series: This series is also known as the 4n chain of Th-232 or thorium cascade. The series started from thorium-232 through radium, actinium, radon, polonium, bismuth, thallium and ends in lead-208 with total released energy of 42.6 MeV.

Uranium Series: The series is also known as the 4n+2 chain of U-238 or radium series. It started from uranium-238 through thorium, protactinium, radium, radon, polonium, astatine, bismuth, thallium and ends in lead-206 with total released energy of 51.7 MeV.

Actinium Series: This is also called 4n+3 chain of U-235 or plutonium cascade. The series begins with uranium-235 through thorium, protactinium, actinium, radium, francium, radon, astatine, polonium, bismuth, thallium and ends in lead-207 with total released energy of 46.4 MeV.

The radionuclides of U-238, Th-232, and U-235 decay series are shown in figure 2.1 along with the major mode of radioactive decay for each element.

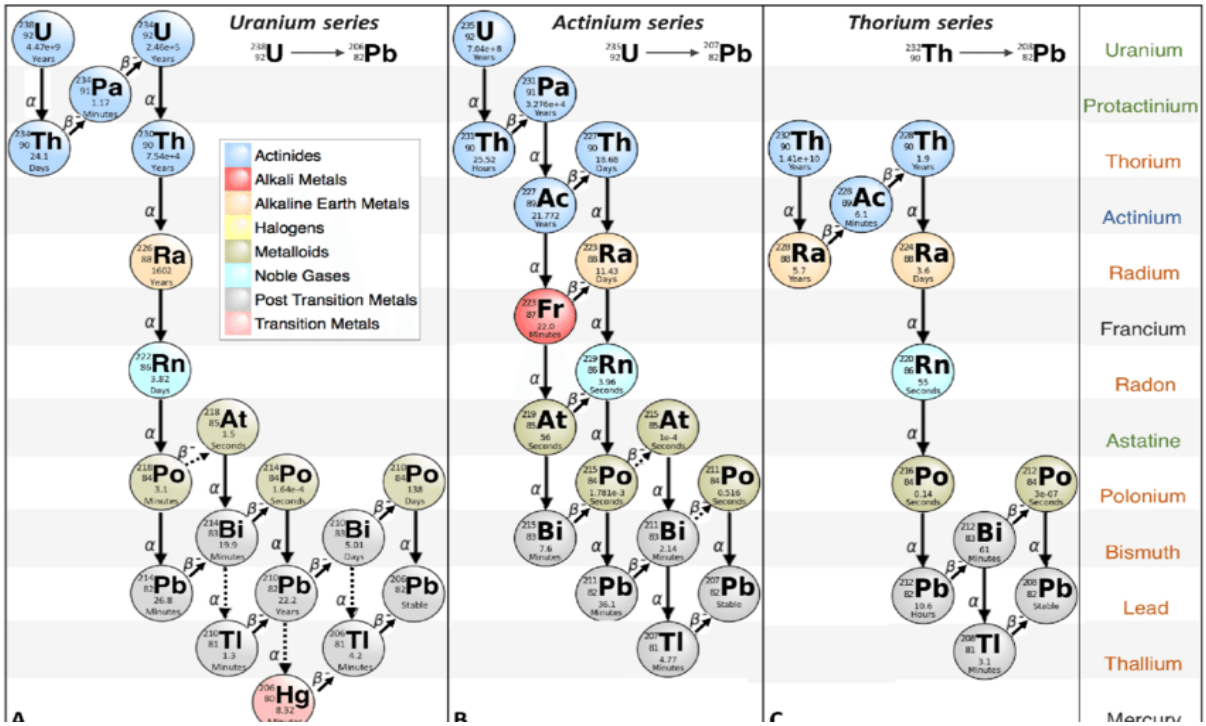


Figure 2.1: Decay series of U-238, U-235, and Th-232
Source: Adopted from www.researchgate.net (2017)

- Potassium-40 (K-40) Decay Scheme:

Potassium is the seventh most abundant element in the Earth's crust, and K-40 averages 850 Bq/kg there. It is found in many foodstuffs (bananas for example), and indeed fills an important dietary requirement, ending up in our bones (UNSCEAR, 2000). Potassium-40 is a radioactive isotope of potassium which has a very long half-life of 1.251 x 10^9 years. Its beta decays, mostly to calcium-40, forms 0.012% of natural potassium which is otherwise made up of stable K-39 and K-41. Figure 2.2 shows the decay chain K-40.

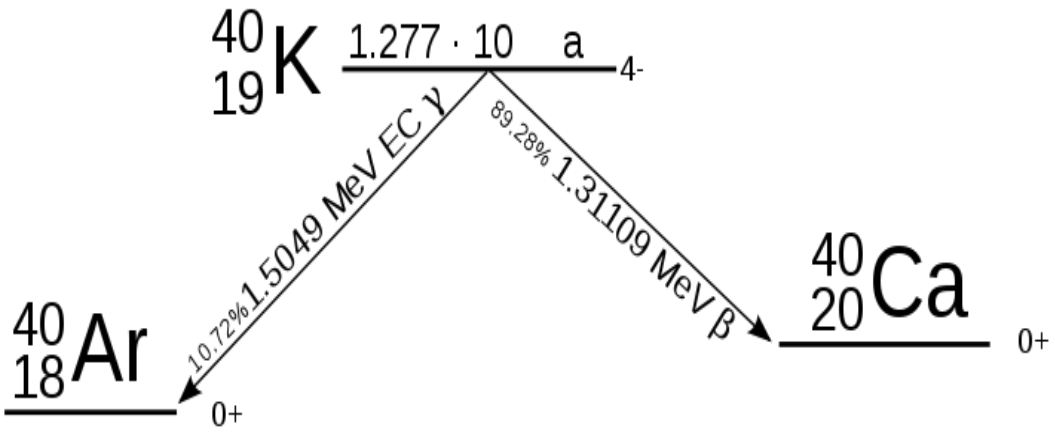


Figure 2.2: Decay chain of K-40

Source: Adapted from www.wikimedia.org (2017)

2.2.1.2 Cosmogenic radionuclides

The Earth and all living things on it are constantly bombarded by cosmic radiation from outer space. This radiation comes from the sun, stars, collapsed stars (such as neutron stars), quasars, and in the hot galactic and intergalactic plasma. This radiation primarily consists of positively charged ions from protons to iron and larger nuclei derived sources outside our solar system. This radiation interacts with atoms in the atmosphere to create an air shower of secondary radiation, including X-rays, mesons, muons, protons, alpha particles, pions, electrons, and neutrons. The immediate dose from cosmic radiation is largely from muons, neutrons, and electrons, and this dose varies in different parts of the world based largely on the geomagnetic field and altitude. The initial energy of the individual particles constitutes a broad spectrum from a few electron volts (eV) to about 1,020 eV. Cosmic radiation loses energy as it penetrates the atmosphere. The protective shield of the atmosphere and the earth's magnetic field prevent the soft energy radiation components from penetrating the atmosphere. The hardest components, the mesons, dominate at sea level. Above about 5 km from the sea level, the electrons are equal or dominate the mesons, whereas above 25 km protons dominate. Cosmic radiation produces X-rays and neutrons as it penetrates through the

atmosphere. Astronomers believe that the contents of natural radionuclides (uranium, potassium, and thorium) as well as the thin layer of atmosphere in the higher altitude regions (mountains) are reasons why they have high levels of human exposure (Shahbazi, 2003; Shahbazi*et al.*, 2013).

2.2.2 Artificial radioactivity

Not all nuclear reactions are spontaneous. Induced radioactivity occurs when stable isotopes are bombarded with particles or radiations. The high neutron flux from nuclear reactors or high energy particles from particle accelerators can cause induced radioactivity (Sidell, 2002). Members of the public have engaged in the use of artificial radionuclides either through medicine or industry.

2.3 Detectors

Radiation detectors are instruments that measure ionization and produce an observable output. Scintillator-type detectors measure the ionizing radiation, using the excitation effect of incident radiation on a scintillator material, and detecting the resultant light pulses. The amplification and storing these data follow the advances in transistor electronics (webmaster, 2000).

As the requirements for greater accuracy, efficiency, or sensitivity increases, so does the complexity of the detector and its operation (webmaster, 2000). For the interest of this study, high purity germanium HPGe detector will be focused on.

2.3.1High purity germanium (HPGe) detector

High-Purity germanium (HPGe) detectors commonly use lithium diffusion to make an n+ ohmic electrode, and boron implantation to make a p+ electrode. Coaxial detectors with a central n+ electrode are referred to as n-type detectors, while p-type detectors have a p+

central electrode (MTI, 2016). They are mostly used for gamma spectroscopy in nuclear physics, as well as x-ray spectroscopy. The germanium has a net impurity level of around 10^{10}atoms/cm^3, so that with moderate reverse bias, the entire volume between the electrodes is depleted, and an electric field extends across this active region. This means that the material has a higher resistivity which is proportional to the square of the manufacture of larger and much more efficient detector (Khandaker, 2011).

The major characteristics of the HPGe detectors are high resolution, low impurity concentration (large depletion depth), low ionizing energy required to produce an electron hole pair, and relative simplicity of operation (Khandaker, 2011).

2.3.2Operations of HPGe detectors

When radiation interacts with the electric field of the active region of HPGe detector, it produces charge carriers which are swept by the electric field to their collecting electrodes, where a charge sensitive preamplifier converts this charge into a voltage pulse proportional to the energy deposited in the detector (MTI, 2016).

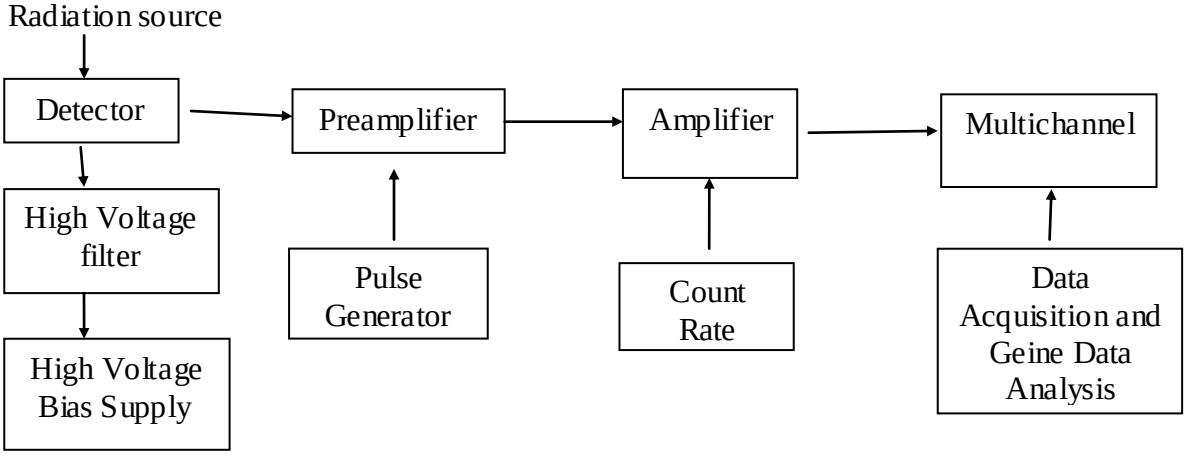


Figure 2.4: Block diagram of the HPGe detector setup (Hossain*et al.*, 2012)

2.3.3 Energy resolution and efficiency of HPGe

The energy resolution and efficiency of the HPGedetector is determined by using standard sources Co-60 and Cs-137. The average value of full width at half maximum (FWHM), corresponds to the resolution of the detector. The FWHM of HPGe increases with increasing in gamma ray energy. That is, resolution is directly proportional to the gamma ray energies. HPGe has better resolution than NaI(Tl) even though both detectors show similar trends with FWHM increasing with gamma ray energy and is a good instrument for nuclide identification. It offers the advantage of resolving two closely located energy points and has the ability to detect a mixture of nuclear material (Hossain*et al.*, 2012).

The detection efficiency is a measure of the percentage of radiation that a given detector detects from the overall yield that is emitted from the source into a solid angle of usually 4π in the photo-peak. It has been shown that efficiency decreases exponentially with increases in gamma ray energy. HPGe detector has less efficiency compare to the NaI(Tl) detector. It means that, HPGe is efficient in detecting nuclides with lower energy but not nuclides at higher energy. NaI(Tl) detector is more efficient detector than HPGe detector, although it has a very poor resolution (Hossain*et al.*, 2012).

2.4 Review of Previous Works

The study of environmental natural radioactivity and the potential risk of exposure have been the interest of some researchers in the recent times.

In Malaysia, Garba*et al.*, (2016a) measured terrestrial gamma radiation dose (TGRD) rate from 35 to 340 nGy/h with mean value of 150 nGy/h and the annual effective dose to the populace was 0.92 mSv/y. They revealed the mean (range) activity concentration of Ra-226, Th-232, and K-40 in the soil samples were 79 $\pm$ 3 (20 $\pm$ 1 to 151 $\pm$ 5) Bq/kg, 8 $\pm$ 3 (8 $\pm$ 1 to 182 $\pm$ 6) Bq/kg, and 545 $\pm$ 55 (47 $\pm$ 1 to 1056 $\pm$ 107) Bq/kg respectively and concluded that

the mean activity concentrations of Ra-226 and Th-232 in the soil of Terengganu are higher than the world averages by a factor of two, while that of K-40 is approximately 15% higher than the world average.

Garba*et al.*, (2016b) in their radiological mapping of Kelantan, Malaysia, using a portable hand-held radiation survey meter and global positioning system found the mean (range) TGRD as 209 nGy/h(300 - 500 nGy/h). The measurements were done based on geological formations and soil types of the area.

Garba*et al.*, (2015) carried out measurement of terrestrial gamma radiation dose (TGRD) rates in 145 different locations of Terengganu State, Malaysia using NaI(Tl) micro roentgen survey meter and found that the TGRD rates ranged from 35 to 340 nGy/h with mean value of 150 nGy/h. The annual effective dose to population was found to be 0.92 mSv/y. The data obtained were used in constructing the gamma isodose map using ArcGIS 9.3 version which shows the distribution of TGRD rates across the state.

Zeb*et al.*, (2015) carried out survey of gamma radiation exposure around Pakistan Institute of Nuclear Science and Technology (PINSTECH) and found that the average outdoor absorbed dose rate in air as 59$\pm$ 16 nGy/h, average annual outdoor dose rate due to terrestrial gamma rays as 71.4$\pm$ 20.0 μSv/y. The estimated annual collective effective dose equivalent is 415 manSv and excess lifetime cancer risk is 7.3 x10^{-4}.

Patil*et al.*, (2015) carried out radiological mapping of Bhubaneswar City with compact Aerial Radiation Monitoring System (CARMS), Gamma Tracer (GT), μR Survey Meter and Identi-Finder and found that the dose rate ranged between 90 – 130 nSv/h,. The study confirmed the presence of Th-232, Ra-226, and K-40 in the City.

Nabil *et al.*, (2015) studied the radionuclides concentrations of U-238, Th-232, and K-40 in phosphate ore and fertilizer in Egypt and found them as 871 ± 91.90 Bq/kg, 19.21 ± 2.42 Bq/kg, and 176.66 ± 17.66 Bq/kg respectively with calculated values of the radiological hazards of the radium equivalent activity, external and internal indices, and annual effective dose.

Gabdo*et al.*, (2014) carried out radiological study to determine the health hazard associated with concentrations of natural radionuclides Ra-226, Th-232, and K-40 in soils of northern part of Pahang State, Malaysia and found the mean terrestrial gamma dose rate (TGDR) to be 185 ± 7 nGy/h, the mean activity concentrations of radionuclides of Ra-226, Th-232, and K-40 to be 117 ± 4, 151 ± 5, and 622 ± 57 Bq/kg respectively, and the Radium equivalent activities, external hazard index, and annual effective dose for outdoor measurements to be 380 Bq/kg, 1.027 and 0.210 mSv/y respectively.

Sharma *et al.*, (2014) in their direct measurement of absorbed dose rate in air due to exposure from outdoor terrestrial radiation showed that the absorbed dose rates in air ranged between 81.33 ± 2.34 nGy/h to 144.00 ± 5.77 nGy/h, annual effective dose rate ranged between 0.10 ± 0.012 to 0.18 ± 0.007 mSv/y, and excess lifetime cancer risk is in range of 0.375 $x10^{-3}$ to 0.662 $x\ 10^{-3}$ for the outdoor measurements.

Aznan*et al.*, (2009) carried out research to investigate the levels of natural radioactivity and the associated radiation hazard in some Malaysia's sand used in building constructions and found the activity concentrations of Ra-226, Th-232, and K-40 range from 6.45 to 107.90 Bq/kg, 7.78 to 96.67 Bq/kg, and 31.05 to 1105.53 Bq/kg respectively, with mean range of annual equivalent doses to dwellers were in the range of 0.059 ± 0.005 to 0.738 ± 0.018 mSv/y and the range of representative gamma level indices as 0.189 ± 0.027 to 2.366 ± 0.057.

In Nigeria, Isinkaye and Emelue, (2015) assessed the distribution of naturally occurring radionuclides Ra-226, Th-232, and K-40 and evaluation of radiological hazards in sediments of Oguta Lake, South-East Nigeria revealed the mean activity concentrations of Ra-226, Th-232, and K-40 were 47.89 ± 18.67 Bq/kg, 55.37 ± 32.74 Bq/kg and 1023 ± 474 Bq/kg respectively. The results of the radiological indices and dose rates were not higher than the maximum recommended limits indicating that the uses of the sediments as building materials do not constitute any excessive radiological hazards.

In a research conducted by Osimobi*et al.*, (2015) on GIS mapping and background ionizing radiation (BIR) levels in the sites range from 0.012 to 0.028 mR/h, while the corresponding calculated equivalent dose rate ranged from 1.0 mSv/y to 2.35 mSv/y with a mean value of 1.51 ± 0.04 mSv/y. This shows that the average exposure level of the studied area is 38.5% higher than the international standard.

Avwiri*et al.*, (2014) carried out study to estimate the radiation health hazard indices and excess lifetime cancer risk associated with exposure to river water, soil and sediments from Mini-Okoro/Oginigba Creek, Port Harcourt, Rivers State and revealed that the activity concentrations of U-238, Th-232, and K-40 in all samples were within the world acceptable values, but was higher than the result of other works carried out in similar environment. They further said the contributions of U-238, Th-232 and K-40 to the effective dose were 56.9%, 27.2%, and 15.9% respectively in water, 33.6%, 21.2%, and 45.2% respectively in sediment and 71.8%, 14.2%, and 14.0% respectively in soil and concluded that there is no immediate radiation health hazard associated with the use of any of the samples studied.

Girigisu*et al.*, (2013) carried out study on assessments of radiological levels from Bagega artisanal gold mining exercises in Zamfara State, Nigeria and revealed the mean activities of K-40, Ra-226, and Th-232 are 370.79 ± 7.98 Bq/kg, 18.3 ± 1.77 Bq/kg, and 16.86 ± 0.94

Bq/kg respectively with mean value of outdoor gamma and annual effective dose rates as 27.25 nGy/h and 0.033 mSv/y respectively. Though the results show low radiological exposure, but the non-usage of gas mask by artisans put them at risk of exposure to respiratory crystalline silica as well as exposure to radon gas inhalation.

Avwiri*et al.*, (2012) conducted research to evaluate the radiation hazard indices and excess lifetime cancer risk due to natural radioactivity in soil profile of Udi and Ezeagu local government areas of Enugu State, Nigeria and found the average concentrations of K-40, Ra-226, and Th-232 as 57.17 Bq/kg, 13.71 Bq/kg and 10.09 Bq/kg respectively for the first well and 59.77 Bq/kg, 11.49 Bq/kg and 8.83 Bq/kg respectively for the second well and concluded that radiation exposure to the residents of the studied areas pose no significant health threat to the residents.

In view of these, this study is undertaken to assess environmental radiological status of Northern Zamfara State, Nigeria.

CHAPTER THREE

METHODOLOGY

3.1 Materials

The materials used in this study are listed below:

- Radiation Survey Meter (Inspector Alert^{TM} Nuclear Radiation Monitor, Serial Number: 35440), Manufactured by Iospectra U.S.A.
- Global Positioning System (GPS) MAP78 by GARMIN
- Digital Weighing Balance (GF-200) built by A&D instruments LTD, Japan.
- Gallenhamp Oven BS (Serial Number: 054334) built by Unified National Inventory Database.
- Coaxial p-type HPGe detector (Model: GC 8023, Serial Number: 9744) manufactured by Canberra.
- Cutlass
- Masking Tape
- Marker
- Polyethylene Bags
- Disposable Hand Gloves
- Sieve
- Plastic Containers
- Petroleum Jelly
- Candle wax

3.2 Study Area

The study area covered the seven (7) local government areas (Bakura, Maradun, Shinkafi, Zurmi, KauraNamoda, BiriniMagaji and TalataMafara) of Northern Zamfara State, which lies within the longitudes 5°00′E and 7°15′E, and the latitudes 12°00′N and 13°15′N (Figure 3.1).

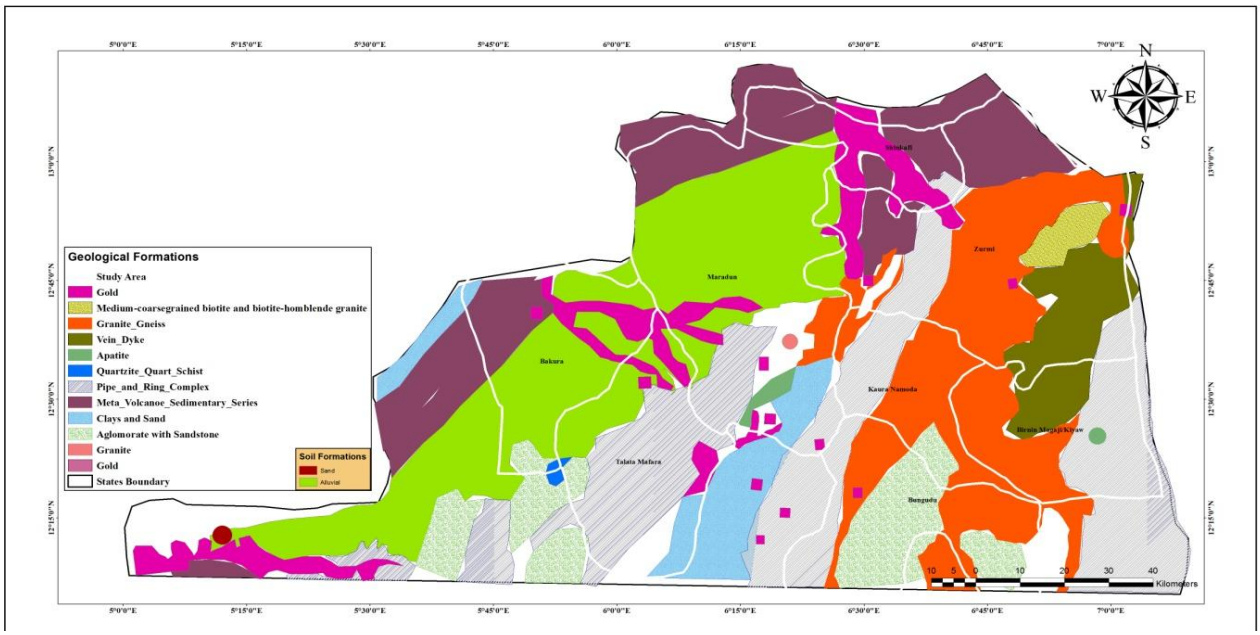


Figure 3.1: Digitized geological map of the study area (NGSA, 2013).

3.2.1 Geology of the study area

Geological land formations play an important role in the life of all people and human development. They influence the region's cultural history, where people chose to live, the kind of crop they grow, their societal development, architectural choices and building development (Laurie, 2018). The study area is underlain by five geological formations: Gneiss-Migmatites, Old Metasediments and Older Granite formations, formed from the Precambrian to Cambrian time, Guadumi/Illo and Taloka formations of the Cretaceous age, and alluvium of the recent age (NGSA, 2013). The granites, gneisses and migmatites are likely resistant to erosion, but when weathered result into poor soils. The metasediments, on the other hand, consist of phyllites, quartzites and meta-conglomerates (NGSA, 2013;

Innocent *et al.*, 2014) which when weathered give rise to more fertile soils. This accounts the fact that the schists are rich in magnesium minerals.

A generalized succession of the geological formations of the NorthernZamfara State from the Precambrian era to the recent is summarized in the Table 3.1.

Table 3.1: Successions of geological formations and their rock types (NGSA, 2013).

Age	Geological formations	Rock types
Precambrian to Cambrian	Gneiss – Migmatite	Granite gneiss, Migmatite, and Banded gneiss.
	OldMetasediments	Meta-gabbro, Schists, Muscovite, Quartzite, Slate, Phyilite, Corbonaceous, Amphibolite, Metasandstone, Metaconglomerate.
	Older Granite	Diorite, Granite andBiotite.
Cretaceous	Gundumi/Illo	Clays grits, Pebbles, Gravels and Sand.
	Taloka formation	Sandstones, clays, shales, sand and tuff with sandstones.

3.3 Terrestrial Gamma Radiation Dose (TGRD) Rate Measurements

The terrestrial gamma radiation dose rates of the study area were measured with a handheld radiation survey meter (Inspector Alert^{TM} Nuclear Radiation Monitor manufactured by International Medcom, Inc, United States of America). The survey meter uses a halogen-quenched Geiger-Muller tube, effective diameter of 45 mm with mica window density 1.5 – 2.0 mg/cm^2. Its gamma sensitivity was 3500 CPM per 1 mR/h referenced to Cs -137. The Geiger-Muller tube generates a pulse of electrical current each time radiation passes through the tube and causes ionization. Each pulse is electronically detected and registers as a count.

The meter displays the counts in the mode you choose: counts per minute (CPM), counts per second (CPS), milli roentgens per hour (mR/h) or micro sievert per hour (μSv/h) (IMI, 2015).

3.3.1 Calibration of the Inspector Alert Meter

Calibration of the Inspector Alert Meter is best done by using a calibrated source of standard radionuclide, Cesium-137. Before calibrating, it was ensured the distance between the meter and the source was correct to produce the appropriate dose rate. The meter was turned off and the Mode Switch was set to mR/h. Then, the end panel ON button was held down while the meter was switched on. The meter displayed CAL, and beeped each second for 15 seconds before exposing the standard source.The meter collected data for 30 seconds, beeping once every second. At the end of the 30 seconds, the meter beeped several times and displayed CAL and SET. The + and – buttons were used to adjust the reading to standard (100) and Set Button was used to accept the new reading, and new calibration factor was automatically calculated from the adjustment made. The new calibration factor was displayed for several seconds, and the meter beeped and resumed its regular operation (IMI, 2015).

3.3.2 Measuring with the Inspector Alert Meter

The survey meter was held at 1 m above the ground level. The number of counts detected by the Inspector Alert varies from reading to reading due to the random nature of radioactivity. A reading is expressed more accurately as an average over time, and the average is more accurate over a longer time period (IMI, 2015). For this reason, five readings were taken from each point to minimize error. The readings were taken in milli-Roentgen per hour (mR/h) and were later converted to nano-Gray per hour (nGy/h) with the conversion factor of 1 mR/h = 1428.57nGy/h. A Global Positioning System, Garmin (GPS Map78) was used to record the coordinates of each location. The measurements were carried out in 166 different locations randomly (Figure 3.2).

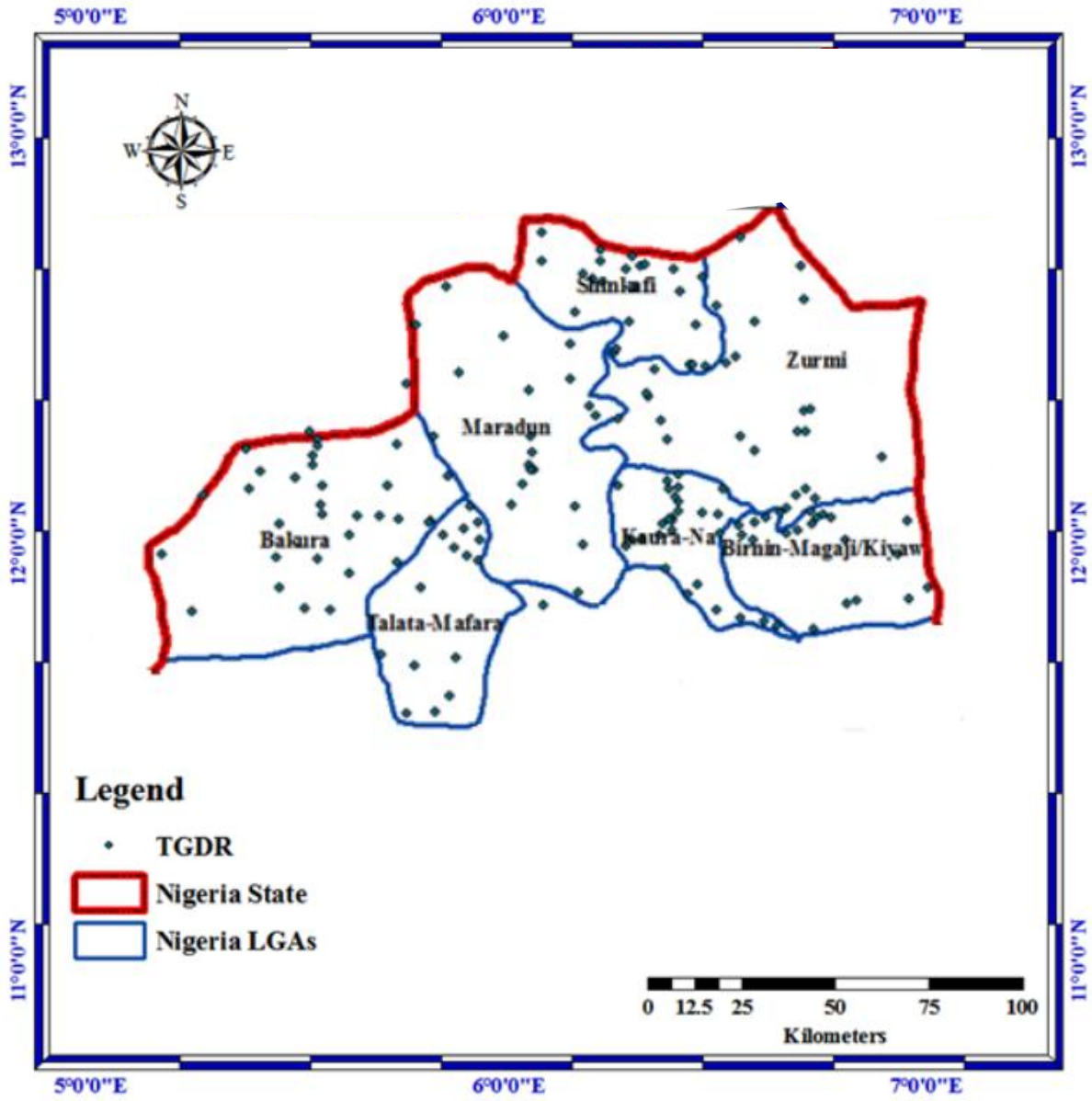


Figure 3.2: Location points of Gamma Dose Rates Measurements

3.4 Radiological Mapping

The knowledge of terrestrial gamma radiation dose (TGRD) is very important in Health Physics. TGRD map is very important in determining the radiological status of an area (Gabdo*et al.*, 2014). Radiological mapping of the study area was plotted using ArcGIS software version 10.3. The coordinates of each point were recorded in degree minute second

unit. The World Geodetic System of definition was used in defining the coordination system (Garba*et al.*, 2014).

3.5 Soil Sample Collection

Sampling points were marked on the geological map of the study area before visiting the site. The marking were based on the geological formations (Figure 3.1). On the site, the coordinates of the sampling points were traced and recorded using a Global Positioning System (GPS) MAP78 manufactured by GARMIN. Eighteen soil samples covering the entire geological formations were collected and packed into a well-labelled polyethylene bags (Table 3.2). The samples were taken from the depth of 20.0 – 50.0 cm within a diameter of 50.0 cm in an open field. Each polythene bag was sealed to avoid cross contamination with other samples during transportation to the laboratory for further preparations.

Table 3.2: Sample labels of each geological formation

Geological Formations	Sample ID
Gneiss-Migmatite	GM1, GM2, GM3 and GM4.
OldMetasediments	OM1, OM2, OM3 and OM4
Older Granite (Pan-African)	OG1, OG2, OG3 and OG4
Gundumi/Illo Formation	GF1, GF2, GF3, and GF4
Taloka Formation	TF1 and TF2

3.6 Sample Preparation

The soil samples were dried with a Gallenhamp Oven built by Unified National Inventory Database, at temperature range of 100^{o}C to 120^{o}C for 12hrs to remove any available moisture in the samples at Material Science Laboratory, Department of Physics, Ahmadu Bello

University Zaria. The dried samples were crushed and sieved into a fine powder with a sieve mesh of about 250 μm for homogeneity. The homogenized samples were then weighted 500g each and sealed into cylindrical plastic containers, and were taken to the National Institute of Radiation Protection and Research (NIRPR), University of Ibadan.

At NIRPR laboratory, the samples were packed into standard 500 ml Marinelli beakers and undergo three sealing stages to prevent radium-222 from escaping. Firstly, the inner rims of the Marinelli beakers lid were smeared with petroleum jelly and placed in position to fit. Secondly, the beakers lids were sealed up with candle wax to avoid gaps. And finally, each lid was fastened on its beaker with a masking adhesive tape. The sealed samples were stored for a minimum period of 30 days, so as to allow radium and its progeny attain secular equilibrium. This method was adopted by other scholars (Innocent *et al.*, 2014, Ibrahim *et al.*, 2015, Raghu *et al.*, 2015,Garba*et al.*, 2016).

3.7 Experimental Set-Up

A coaxial p-type high purity germanium (HPGe) gamma-ray spectrometry set-up manufactured by Canberra (Model: GC 8023; Serial Number: 9744) with end cap diameter of 78 mm and length of 69.8 mm, a relative efficiency of 80% and an energy resolution (FWHM) of 2.3 keV for the 1.33 MeV gamma-ray emission of Co-60, connected to a personal computer-based data acquisition system, which has Genie 2000 (VI.3) software from Canberra and 16,000 Multi-Channel-Analyzer located at NIRPR laboratory, University of Ibadan was used to analyze the samples.

The energy was calibrated using the standard sources of Co-60 (1173.2 and 1332.5keV), Am-241 (59.54keV), Ba-133 (356.1keV), Cs-137 (661.9keV), and Na-22 (1368.6keV), whereas the peak efficiency was calibrated using Eu-155 (60 keV, 86.5 keV, and 105.3 keV), Sb-125

(176.3 keV, 427.9 keV, and 600.6 keV), Mn-54 (834.8 keV), Zn-65 (1115.5 keV), and K-40 (1460.8 keV) (MTI, 2016).

3.8 Sample Analysis

The samples were placed on the HPGe detector and each sample was set to counting time of 10,800s, which was long enough for the detector to analyze the spectrum with the peaks of interest clearly shown and well distinguished. The background count was estimated by empting the container and count in a closed detector using the same container lid geometry as in the previous count. This procedure was maintained throughout the analysis. The count rate in count per second (CPS) was obtained for each radionuclide in every sample analyzed and the background count was subtracted for every count.

U-238 count rate was measured from 351.9keV gamma-ray peaks of Pb-214 and 609.31 keV and 1120.3 keV gamma-ray peaks of Bi-214. Th-232 count rate was estimated from the 911.1 keV gamma-ray peak of Ac-228 and 583.19 keV and 2614.53 keV of Tl-208. K-40 count rate was estimated using the 1460 keV gamma-ray peak from K-40 itself.

3.9 Activity Concentration

The count rate under the photo-peak of each of the primordial radionuclide was converted to activity concentration, A using the equation 3.1 (Isinkaye and Emelue, 2015):

$$\text{A (Bq/kg)} = \frac{C}{\varepsilon PTM} \tag{3.1}$$

where$C$ is the count rate under the corresponding photo-peak, ε is the absolute efficiency of detector. P is the absolute transition probability of the specific gamma-ray, and M is the mass of each sample in kg and T is the live time of measurement (sec).

3.10Radiological Hazards

The potential radiological hazards associated with the environment were assessed by estimating the Radium equivalent activity (Ra_{eq}), external hazard index (H_{ex}), the absorbed gamma dose rate (D_R), the annual effective dose rate (H_R), the activity utilization index (AUI), and the excess lifetime cancer risk (ELER).

3.10.1 Radium equivalent activity (Ra_{eq})

Radium equivalent activity (Ra_{eq}) is defined as the activity concentration of a radionuclide equivalent to 370Bq/kg of U-238, which gives outdoors and external effective dose rate of 1.5mGy (1mSv) per year (Tufail, 2012). It is a radiological parameter that compares the activity concentrations of U-238, Th-232, and K-40 (Isinkaye and Emelue, 2015) and has been in use to assess the radiological hazard of radioactivity for the past four decades (Tufail, 2012). The relationship between the radium equivalent activity and the activity concentrations of the three primordial radionuclides of U-238, Th-232, and K-40 is described by equation 3.2 (Innocent *et al.*, 2014, Nabil *et al.*, 2015, Raghu *et al.*, 2015, Garba*et al.*, 2016):

$$Ra_{eq} = A_U + 1.43A_{Th} + 0.077A_K \quad (3.2)$$

where A_U, A_{Th}, and A_K are the activity concentrations of U-238, Th-232, and K-40 respectively.

This estimation is based on the ground that 1 Bq/kg of U-238, 0.7 Bq/kg of Th-232 and 13 Bq/kg of K-40 produce the same gamma-ray dose rate. This index (Ra_{eq}) is related to both internal doses due to the radon and external gamma dose (Raghu *et al.*, 2015) and should not be greater than 370 Bq/kg, the world average for a safety environment (UNSCEAR, 2000).

3.10.2 External hazard index (H_{ex})

External hazard index (H_{ex}) is an assessment of the external exposure level due to gamma radiation. This determines the dose delivered externally to individuals from the environment. It was estimated using equation (3.3)(Innocent *et al.*, 2014, Raghu *et al.*, 2015, Garba*et al.*, 2016):

$$H_{ex} = \frac{A_U}{370Bq\ /kg} + \frac{A_{Th}}{259Bq\ /kg} + \frac{A_K}{4810Bq\ /kg} \quad (3.3)$$

where $A_{U,}$, A_{Th}, and A_k are activity concentrations of U-238, Th-232, and K-40 respectively in Bq/kg. The value of this H_{ex} should be less than unity, if not the environment is not safe (UNSCEAR, 2000).

3.10.3 Activity utilization index (AUI)

Activity utilization index is a radiological health assessment, usually calculated in order to determine the dose in air from different combinations of the various radionuclides present in the soil samples. This was calculated using equation (3.4)(Isinkaye and Emelue, 2015):

$$AUI = 0.462\ (\frac{A_U}{50Bq\ /kg}) + 0.604\ (\frac{A_{Th}}{50Bq\ /kg}) + 0.041\ (\frac{A_K}{500Bq\ /kg}) \quad (3.4)$$

where A_U, A_{Th}, and A_K are the concentrations of U-238, Th-232, and K-40 in Bq/kg respectively and 0.462, 0.604, and 0.041 are the fractional contributions to the total dose rate in air due to gamma radiation from the actual concentrations of these radionuclides.

3.10.4 Absorbed gamma dose rate (D_R)

Absorbed dose is the concentration of energy deposited in a matter as a result of exposure to ionizing radiation, that is, the amount of energy deposited per unit mass of matter. This is usually expressed in unit as J/kg or gray (Gy). Therefore, absorbed gamma dose rate (D_R) is

the amount of radiation delivered over a period of time. This was estimated through the equation (3.5) (UNSCEAR, 2000, Innocent *et al.*, 2014, Garba*et al.*, 2016):

$$D_R\ (nGy/h) = 0.462\frac{nGy\ /h}{Bq\ /kg}\ A_U + 0.604\frac{nGy\ /h}{Bq\ /kg}A_{Th} + 0.0417\frac{nGy\ /h}{Bq\ /kg}\ A_K \qquad (3.5)$$

where A_U, A_{Th}, and A_K are the activity concentration of U-238, Th-232, and K-40 respectively in (Bq/kg) and dose coefficients of 0.462, 0.604, and 0.0417 are the converting factors from Bq/kg to nGy/h for U-238, Th-232 and K-40 respectively.

3.10.5 Annual effective dose rate (H_R)

Annual effective dose rate is the assessment of long-term hazard of exposing matter to ionizing radiation. To estimate this, the conversion coefficient from the absorbed dose in air to the effective dose ($0.7\ x\ 10^{-6}$mSv/nGy) and the outdoor occupancy factor (0.2) as proposed by (UNSCEAR, 2000) were used. Therefore, the annual effective dose was calculated from the equations (3.6) (UNSCEAR, 2000; Nabil *et al.*, 2015):

$$H_R(mSv/y) = D_R(nGy/h)\ x\ 8760h/y\ x\ O_{out}\ x\ C\ (\text{for outdoor estimation}) \qquad (3.6)$$

where D_R is the value of absorbed dose rate, C is the conversion coefficient factor, and O_{out} is the outdoor occupancy factor.

3.10.6 Excess lifetime cancer risk (ELCR)

This deals with the probability of developing cancer over a lifetime at a given exposure level. It is presented as a value representing the number of extra cancers expected in a given number of people on exposure to a carcinogen at a given dose. Excess lifetime cancer risk (ELCR) was given by equation (3.7) (Avwiri*et al.*, 2012):

$$ELCR = H_R\ x\ DL\ x\ RF \qquad (3.7)$$

where H_R is the annual effective dose rate, DL is average Duration of life (estimated to be 70 years), and RF is the Risk Factor, i.e. fatal cancer risk per Sievet assumed to be 0.05 Sv^{-1} in this study as per ICRP-106 (ICRP, 2008).

CHAPTER FOUR

RESULTS AND DISCUSSIONS

This study aimed at assessing the environmental radiological status of NorthernZamfara State, Nigeria has successfully measured the TGRD rates in the air and activity concentrations of U-238, Th-232, and K-40 in the soil, with respect to the geological formation of the area. The collected samples wereprepared and analysed at the Material Science Laboratory, Ahmadu Bello University, Zaria and National Institute of Radiation Protection and Research (NIRPR) Laboratory, University of Ibadan respectively. The radiological hazards such as the absorbed gamma dose rate, annual effective dose rate, radium equivalent activity, external hazard index etc., were calculated. The results obtained were presented and discussed in this chapter in tables and figures.

4.1 Measurement of TGRD Rates

The measured TGRD rate ranged from 20.00 to 61.00 nGy/h, with a mean value of 31.99±0.61nGy/h. This is less than the world average value of 59 nGy/h (UNSCEAR, 2000; Garba*et al*., 2016). The mean values of TGRD rates with 95% confidence interval of each of the seven local government areas of the entire studied area are summarized in Table 4.1. From the table, KauraNamoda local government recorded the highest average value of TGRD rate 38.47 nGy/h, followed by BirninMagaji with mean value 34.22 nGy/h, and next by Zurmi local government with mean value 33.35 nGy/h. These high values of TGRD rates in those areas could be attributed to the Older Granite land formation covering about 70% land mass of the three local governments. This formation is associated with igneous rocks of high contents of radioactive elements (UNSCEAR, 2000; Bruce, 2009; Nuhu, 2009). However, Bakura local government recorded the lowest average value of TGRD rate 28.48 nGy/h, followed by Maradun local government with average value 28.74 nGy/h, and next by

Shinkafi local government with average value 29.94 nGy/h. These low values of TGRD rates in these areas could be traced to the Gundumi/Illo land formation covering about 90% land mass of the three local governments. This formation consists of rock types of low contents of radioactive materials (UNSCEAR, 2000;Nuhu, 2009).

Table 4.1: Mean TGRD rates for each of the seven LGAs of the study area.

L.G.A.	N	Terrestrial Gamma Radiation Dose Rate (nGy/h)						
		Mean	Std. Deviation	Std. Error	95% Confidence Interval for Mean		Minimum	Maximum
					Lower Bound	Upper Bound		
Shinkafi	22	29.94	3.881	0.827	28.21	31.66	21	37
Zurmi	23	33.35	11.046	2.303	28.58	38.13	20	61
KauraNamoda	28	38.47	8.136	1.538	35.31	41.62	27	60
BirninMagaji	22	34.22	6.131	1.307	31.50	36.94	24	56
Maradun	26	28.74	4.904	0.962	26.76	30.72	21	40
TalataMafara	14	30.31	7.180	1.919	26.16	34.45	21	50
Bakura	31	28.48	6.377	1.145	26.14	30.82	20	44
Summary	**166**	**31.99**	**7.857**	**0.610**	**30.78**	**33.19**	**20**	**61**

The mean value of TGRD rates with 95% confidence interval of each of the geological formation is presented in Table 4.2. The highest average values of TGRD rates was recorded from Older Granite formation, which could be attributed to the nature of rocks, crustal rocks of high content of radioactive elements (Bruce, 2009; Nuhu, 2009). Meanwhile, the low average values measured from Gundumi/Illo could also be attributed to the nature of their rocks, which host low amount of radioactive elements (Bruce, 2009; Nuhu, 2009). Table 4.3 compares these results with other countries and the world.

Table 4.2: Mean TGRD rates for each of the geological formation

Geological	N	Terrestrial Gamma Radiation Dose Rates (nGy/h)						
					95% Confidence Interval for Mean			
		Mean	Std. Devi.	Std. Error	Lower Bound	Upper Bound	Minimum	Maximum
Taloka formation	22	30.00	5.85	1.25	27.41	32.59	21.43	42.86
Gundumi/Illo formation	61	28.92	5.91	0.76	27.41	30.44	20.00	50.00
Old Metasediments	32	31.29	4.98	0.88	29.50	33.09	21.43	44.29
Older Granite (Pan African)	22	38.90	12.55	2.68	33.33	44.46	22.86	61.43
Gneiss-Migmatite	29	35.47	6.60	1.23	32.96	37.98	20.00	47.14
Summary	**166**	**31.99**	**7.86**	**0.61**	**30.78**	**33.19**	**20.00**	**61.43**

Table 4.3: Comparison of mean TGRD rates of Northern Zamfara with other countries and the world (UNSCEAR, 2000).

Country	Mean TGRD rates (nGy/h)
Nigeria (Northern Zamfara)	**32**
Algeria	61
Egypt	32
Malaysia	92
India	56
China	62
United States	47
Portugal	84
Ireland	42
Poland	45
Greece	56
Russian Federation	65
World	**59**

4.2 Radiological Mapping

A radiological map for the measured TGRD rates was produced using ArcGIS software version 10.3 (Fig. 4.1). From the map, it was observed that about 30% land mass of the studied area were exposure to TGRD rates ranged from 34 to 61 nGy/h. These are areas dominated byOlder Granite and Gneiss-Migmatite formations. While the remaining 70% land mass of the studied area were exposure to TGRD rates ranged from 25 to 34 nGy/h. These are areas dominated byOld Metasediments, Gundumi/Illo and Taloka formations. This observation is in agreement with the result in Table 4.1.

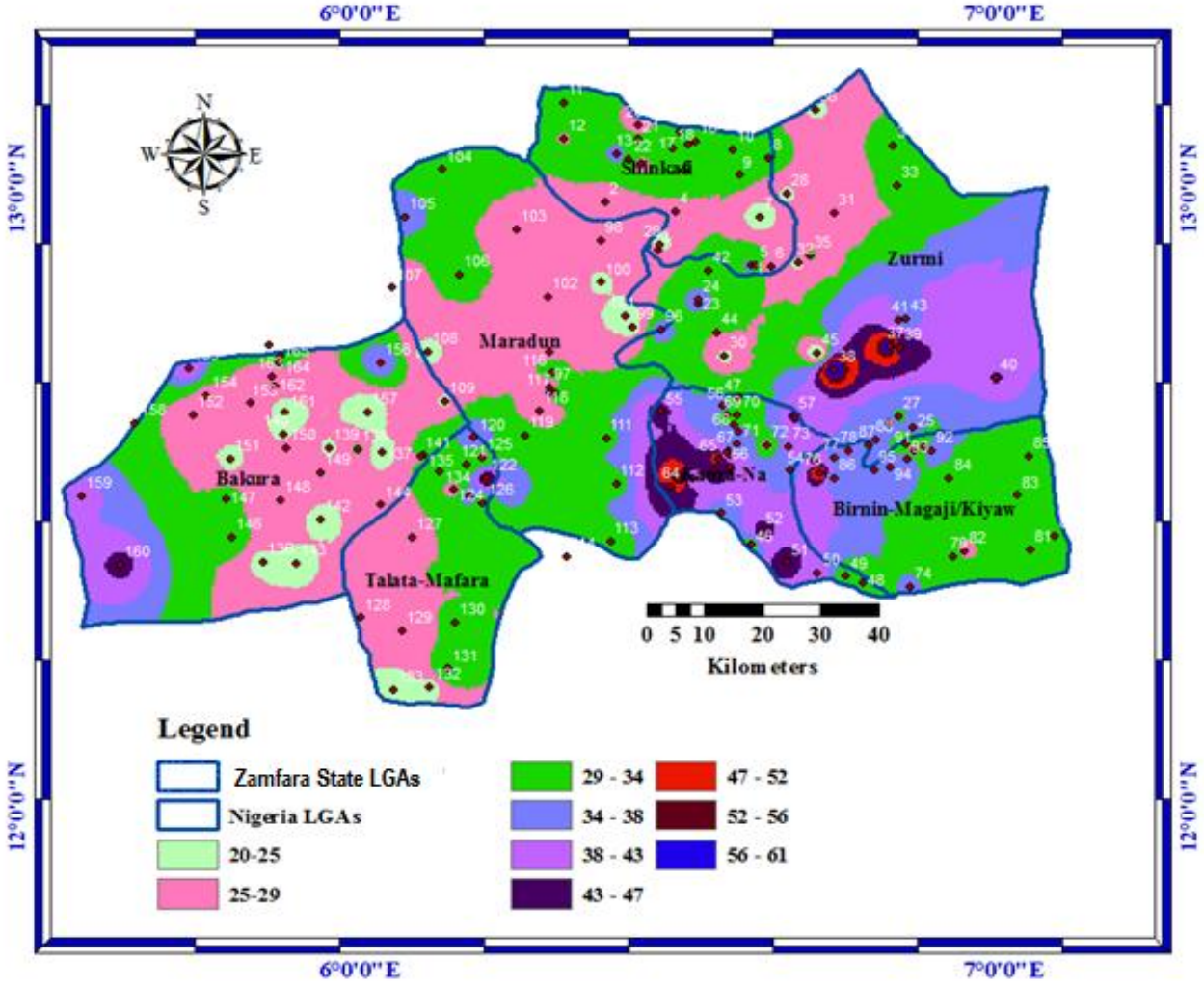


Figure 4.1: A radiological map of the study area.

4.3Activity Concentrations of the Primordial Radionuclides in the Soil Samples

The specific activities of primordial radionuclides were measured for 18 soil samples using HPGespectrometers. The specific activity of the primordial radionuclides of U-238, Th-232, and K-40 in the soil samples ranged from 8.82 ± 0.95 to 44.22 ± 5.78 Bq/kg, 11.02 ± 1.03 to 43.96 ± 4.64 Bq/kg, and 57.45 ± 2.85 to 527 ± 12.38 Bq/kg respectively, with mean values of 19.43 ± 2.22 Bq/kg, 23.26 ± 2.43 Bq/kg, and 268.62 ± 39.03 Bq/kg respectively (Table 4.4). The measured mean activity concentrations of U-238, Th-232 and K-40 in this study were less than the world recommended average.Table 4.5 compares this result with other countries and the world.Figure 4.2 compares the results of the activity concentration of the primordial radionuclides of each of the sample.

Table 4.4: Calculated activity concentrations of U-238, Th-232 and K-40 in the soil.

Geological Formations	Sample ID	U-238 (Bq/kg)	Th-232 (Bq/kg)	K-40 (Bq/kg)
Gneiss-Migmatite	GM1	27.60 ± 2.21	19.75 ± 2.03	488.49 ± 11.73
	GM2	23.38± 1.17	25.71± 2.83	254.84 ± 7.11
	GM3	17.28 ± 2.71	25.56 ± 3.34	493.19 ± 11.15
	GM4	23.50 ± 1.92	32.12 ± 3.82	223.30 ± 6.52
Old	OM1	13.57 ± 0.94	19.28 ± 2.48	163.64 ± 5.40
Metasediments	OM2	20.44 ± 1.12	23.65 ± 2.66	184.34 ± 5.95
	OM3	18.05 ± 0.97	24.55 ± 1.31	145.44 ± 4.72
	OM4	15.26 ± 0.78	18.58 ± 1.34	261.41 ± 7.28
Older Granite	OG1	44.22 ± 5.78	18.23 ± 2.41	527.36 ± 12.38
	OG2	24.91 ± 1.79	37.22 ± 3.02	480.89 ± 11.79
	OG3	19.33 ± 0.88	40.44 ± 3.23	249.25 ± 6.79
	OG4	30.64 ± 3.10	43.96 ± 4.64	481.50 ± 11.27
Gundumi/Illo	GF1	8.82 ± 0.95	11.08 ± 1.03	234.35 ± 6.52
formation	GF2	8.82 ± 0.95	11.08 ± 1.03	234.35 ± 6.52
	GF3	12.36 ± 0.64	14.56 ± 2.01	57.45 ± 2.85
	GF4	10.46 ± 0.99	16.71 ± 7.89	95.15 ± 3.82
Taloka formation	TF1	11.54 ± 1.06	11.25 ± 1.32	117.50 ± 4.31
	TF2	8.95 ± 0.78	12.79 ± 1.19	108.49 ± 4.11
	Range	**8.82 ± 0.95 to 44.22 ± 5.78**	**11.02 ± 1.03 to 43.96 ± 4.64**	**57.45 ± 2.88 to 527.36 ± 12.38**
	Mean	**19.43 ± 2.22**	**23.26 ± 2.43**	**268.62 ± 39.03**

Table 4.5: Comparison of Activity Concentrations in soil of Northern Zamfara with other countries and the world (UNSCEAR, 2000).

Region	Country	Concentration in soil (Bq/kg)					
		K-40		U-238		Th-232	
		Mean	Range	Mean	Range	Mean	Range
Africa	**This work (Northern Zamfara)**	**269**	**57 – 527**	**19**	**9 – 44**	**23**	**11 - 44**
	Egypt	320	29 – 650	37	6 – 120	18	2 – 96
	Algeria	370	66 – 1150	30	2 – 110	25	2 – 140
America	United States	370	100 – 700	35	4 – 140	35	4 – 130
	Costa Rica	140	6 – 380	46	11 – 130	11	1 -42
Europe	Switzerland	370	40 – 1000	40	10 – 150	25	4 – 70
	Russian Federation	520	100 – 1400	19	0 – 67	30	2 – 79
Asia	Japan	310	15 – 990	29	2 – 59	28	2 – 88
	Malaysia	310	170 – 430	66	49 – 86	82	63– 110
World Average		**420**		**33**		**45**	

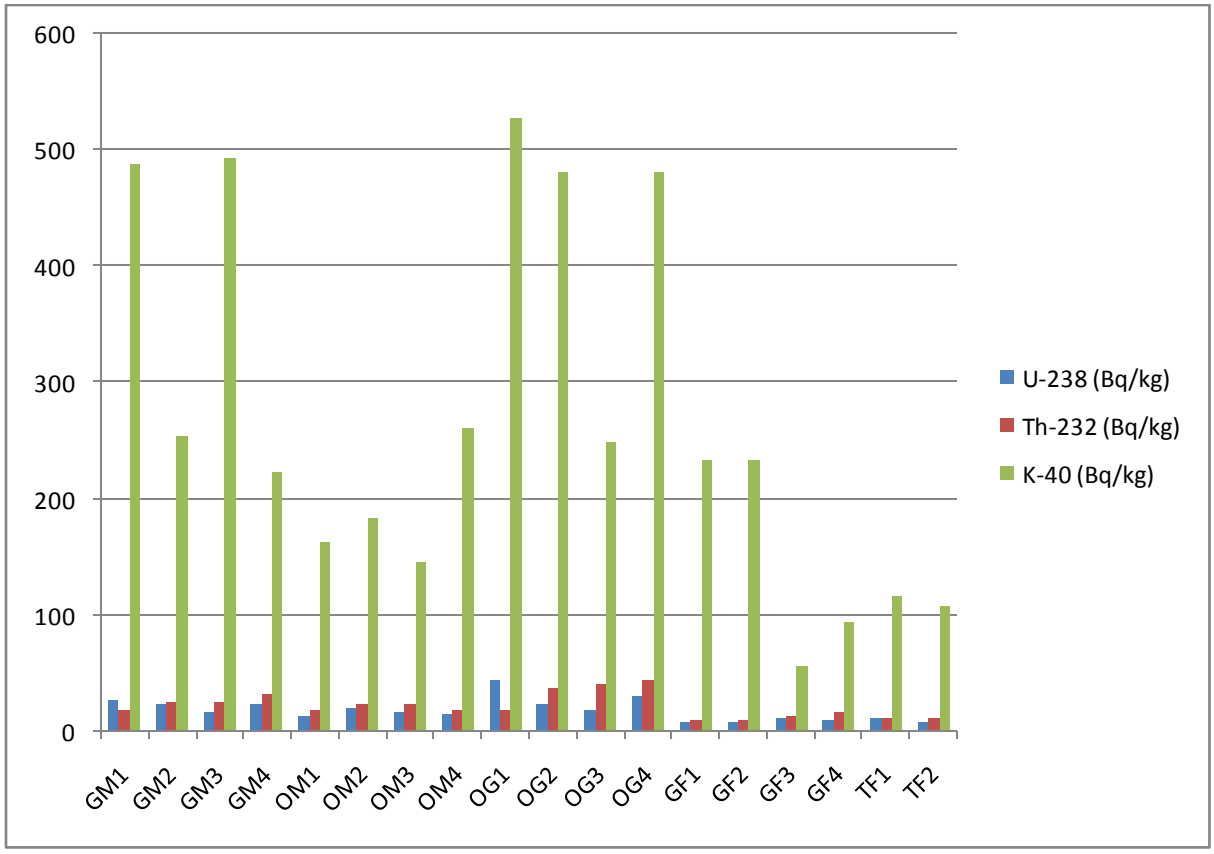


Fig. 4.2: Activity concentrations of U-238, Th-232 and K-40 for each soil sample.

4.4 Radiological Hazards

4.4.1 Radium equivalent activity (Ra_{eq})

The calculated radium equivalent activity ranged from 35.593± 1.899 to 130.578 ± 7.375 Bq/kg, with the average value 71.674 ± 7.099 Bq/kg, which is lower than the safety limit (370 Bq/kg) set for this index so as to keep the annual radiation dose below 2.4 mSv (Garba *et al.*, 2016). Table 4.6 shows the calculated radium equivalent activity of the soil samples. From the table, Older Granite formation recorded the maximum value of radium equivalent activity of 130.578 ± 7.375 Bq/kg from soil sample OG4, whereas Taloka formation recorded least value of 35.593 ± 1.899 Bq/kg. Figure 4.3 compares the results of radium equivalent activity for each of the sample.

Table 4.6: Radium Equivalent Activity

Geological formations	Sample ID	Radium Equivalent Activity (Bq/kg)
Gneiss-Migmatite	GM1	93.456 ± 3.759
	GM2	79.768± 4.248
	GM3	91.806 ± 5.558
	GM4	86.626± 5.812
Old Metasediments	OM1	53.741 ± 3.692
	OM2	68.454± 3.992
	OM3	64.355 ± 2.141
	OM4	61.958± 2.143
Older Granite	OG1	110.896 ± 6.797
	OG2	115.163± 4.762
	OG3	96.351± 4.731
	OG4	130.578± 7.375
Gundumi/Illo formation	GF1	42.709± 1.823
	GF2	42.709± 1.823
	GF3	37.604 ± 2.953
	GF4	41.682± 11.330
Taloka formation	TF1	36.675± 2.190
	TF2	35.593 ± 1.899
	Range	**35.393± 1.899 to 130.578 ± 7.375**
	Mean	**71.674 ± 7.099**

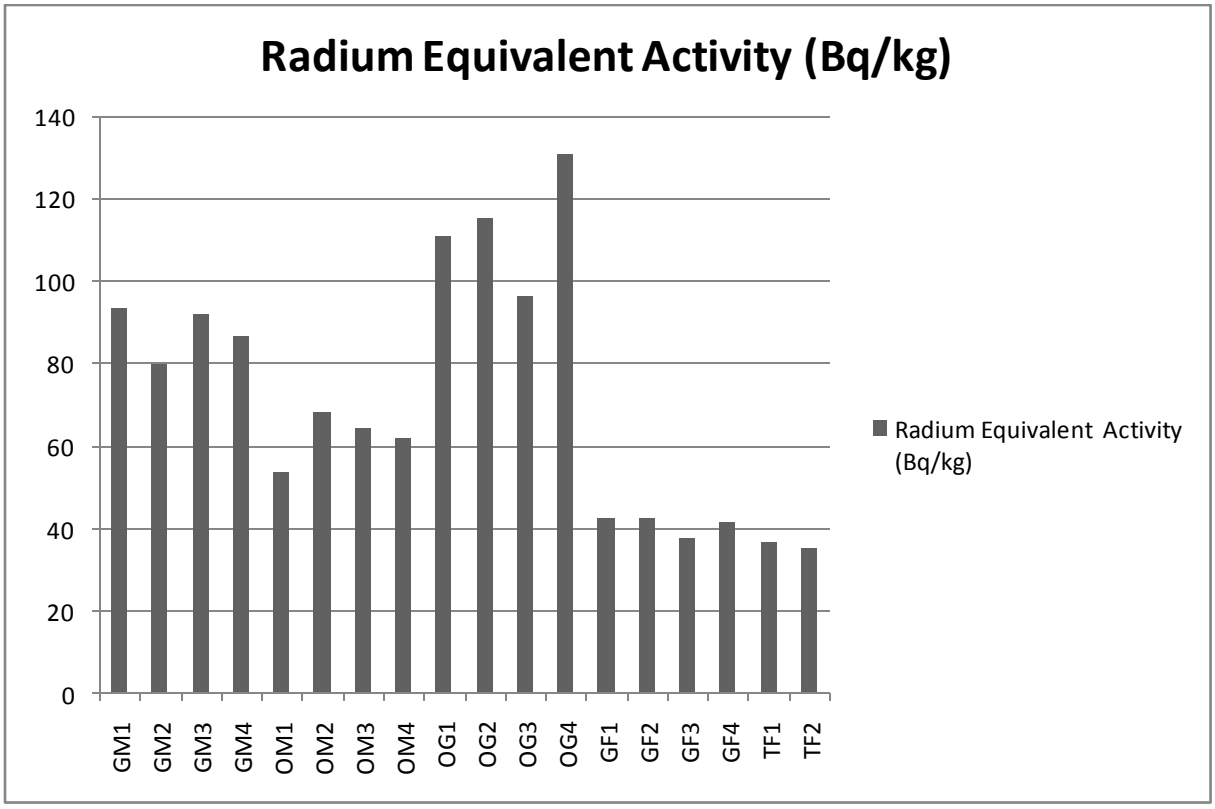


Figure 4.3: Radium Equivalent Activity for each sample

4.4.2 External hazard index (H_{ex})

In this study, the calculated values of external hazard index varied from 0.0961 ± 0.0051 to 0.3526 ± 0.0199, with a mean value of 0.1936 ± 0.0192. This average value is lower than the world recommended maximum unity value for this index. This further confirmedthat the studied area had not been exposed to high gamma radiation dose. Table 4.7 shows the calculated values for this index and figure 4.4 compares the results of this index with each of the sample.

Table 4.7: External Hazard Index

Geological formations	Sample ID	External Index (H_{ex})
Gneiss-Migmatite	GM1	0.2524 ± 0.0102
	GM2	0.2154± 0.0115
	GM3	0.2479 ± 0.0150
	GM4	0.2339± 0.0157
Older Metasediments	OM1	0.1451 ± 0.0100
	OM2	0.1849± 0.0108
	OM3	0.1738 ± 0.0058
	OM4	0.1673± 0.0058
Older Granite	OG1	0.2995 ± 0.0184
	OG2	0.3110± 0.0129
	OG3	0.2602 ± 0.0128
	OG4	0.3526± 0.0199
Gundumi/Illo formation	GF1	0.1153 ± 0.0032
	GF2	0.1153± 0.0032
	GF3	0.1016 ± 0.0080
	GF4	0.1126± 0.0306
Taloka formation	TF1	0.0991± 0.0059
	TF2	0.0961 ± 0.0051
	Range	**0.0961± 0.0051 to 0.3526 ± 0.0199**
	Mean	**0.1936± 0.0192**

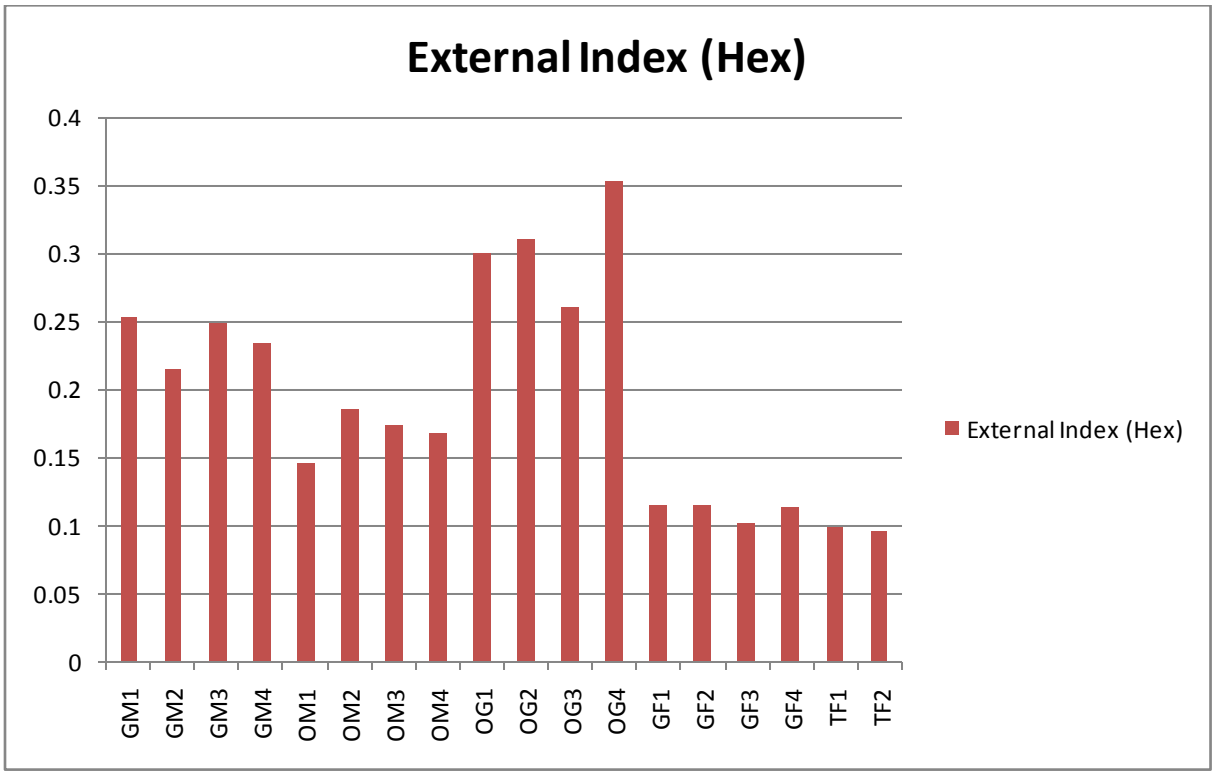


Figure 4.4: External Hazard Index for each sample.

4.4.3 Activity utilization index (AUI)

The estimated activity utilization index ranged from 0.2461 ± 0.0152 to 0.8536 ± 0.0630, with an average value of 0.4688 ± 0.0448. This value is less than 2.0, which corresponds to an annual effective dose less than 0.3 mSv/y. Table 4.8 shows the results of this index, while Figure 4.5 compares the results for each sample.

Table 4.8: Activity Utilization Index

Geological formations	Sample ID	AUI
Gneiss-Migmatite	GM1	0.5337± 0.0319
	GM2	0.5475± 0.0359
	GM3	0.5089 ± 0.0475
	GM4	0.6235± 0.0494
Older Metasediments	OM1	0.3717 ± 0.0312
	OM2	0.4897± 0.0338
	OM3	0.4753 ± 0.0182
	OM4	0.3869± 0.0177
Older Granite	OG1	0.6720 ± 0.0608
	OG2	0.7192± 0.1140
	OG3	0.6876 ± 0.0399
	OG4	0.8536± 0.0630
Gundumi/Illo formation	GF1	0.3246 ± 0.0152
	GF2	0.3246± 0.0152
	GF3	0.2948 ± 0.0250
	GF4	0.3063± 0.0957
Taloka formation	TF1	0.2522± 0.0187
	TF2	0.2461 ± 0.0161
	Range	**0.2346± 0.0152 to 0.8536 ± 0.0630**
	Mean	**0.4688± 0.0448**

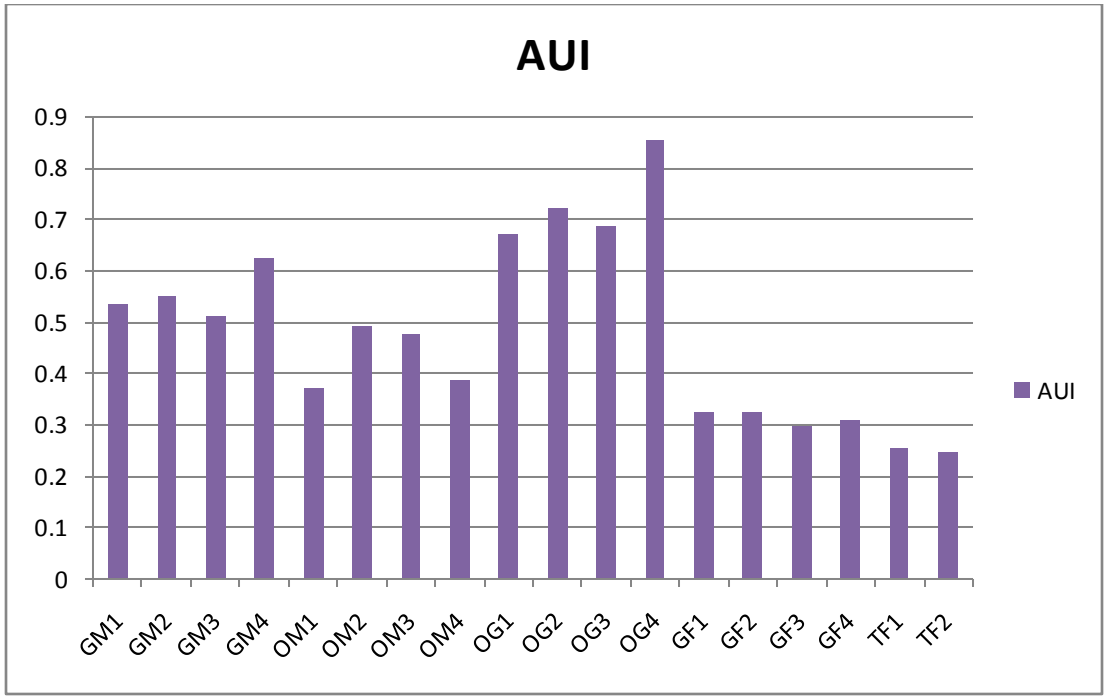


Figure 4.5: Activity Utilization Index for each sample.

4.4.4 Absorbed gamma dose rate (D_R)

The absorbed gamma dose rates in the soil due to the outdoor exposure in the study area have been calculated. The values ranged from 16.384± 0.822 to 60.786 ± 3.182 nGy/h, with an average value of 33.467 ± 3.367 nGy/h. This average value is less than the worldwide average value of 60 nGy/h (UNSCEAR, 2000). Table 4.9 shows the calculated absorbed gamma dose rate of this study, while figure 4.6 compares the results of this parameter for each sample.

Table 4.9: Absorbed Gamma Dose Rate

Geological formations	Sample ID	Absorbed Gamma Dose Rate (nGy/h).
Gneiss-Migmatite	GM1	45.050± 1.669
	GM2	36.957± 1.812
	GM3	43.988 ± 2.419
	GM4	39.569± 3.049
OldMetasediments	OM1	24.738 ± 1.576
	OM2	31.415± 1.706
	OM3	29.232 ± 0.930
	OM4	29.173± 0.937
Older Granite	OG1	53.431 ± 3.084
	OG2	54.042 ± 2.062
	OG3	43.750 ± 2.013
	OG4	60.786± 3.182
Gundumi/Illo formation	GF1	20.540 ± 0.808
	GF2	20.540± 0.808
	GF3	16.900 ± 1.255
	GF4	18.893± 4.790
Taloka formation	TF1	17.026 ± 0.953
	TF2	16.384± 0.822
	Range	**16.384 ± 0.822 to 60.786 ± 3.182**
	Mean	**33.467 ± 3.367**

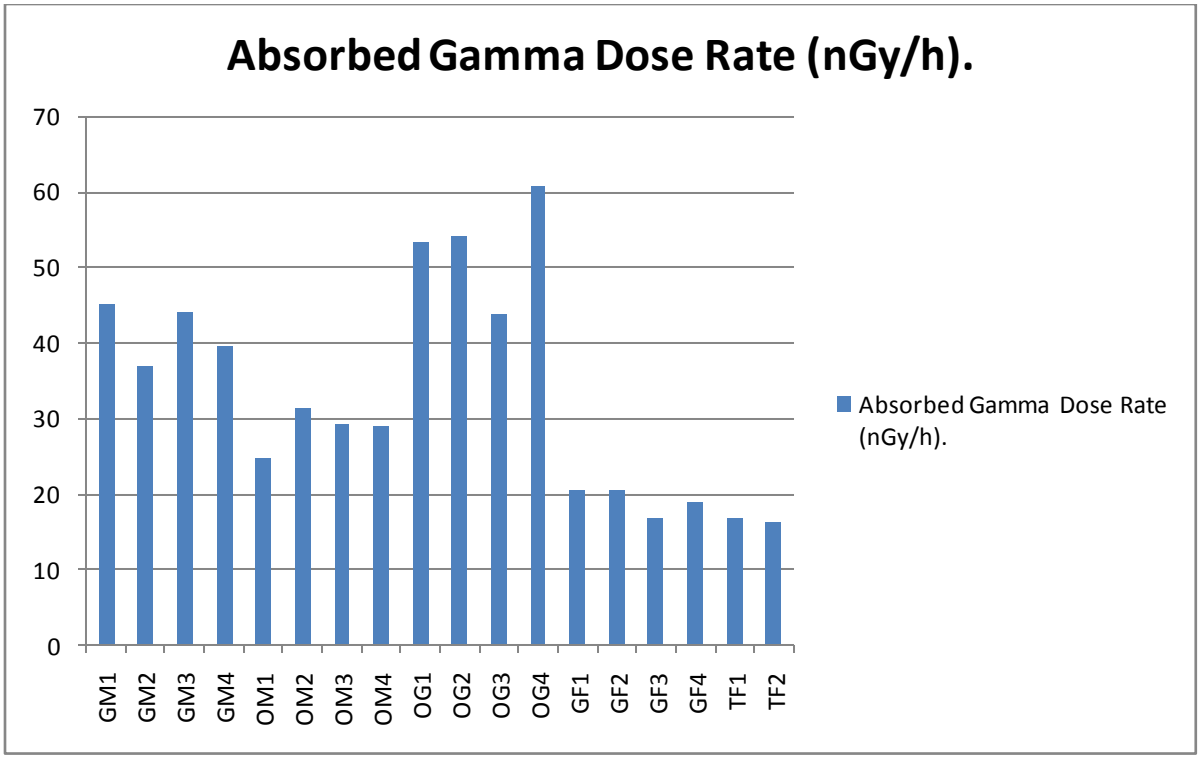


Figure 4.6: Absorbed Gamma Dose Rate for each sample

4.4.5 Annual outdoor effective dose rate (H_R)

The annual outdoor effective dose due to TGRD rates (H_R) in the air was found to be 0.0393 mSv/y. From the spectrometric measurement, it varies from 0.0202 $\pm$ 0.0010 to 0.0748 $\pm$ 0.0039 mSv/y, with an average of 0.0412 $\pm$ 0.0040 mSv/y. The calculated average valuesare less than the worldwide average value of the outdoor annual effective dose rate 0.07 mSv/y (UNSCEAR, 2000). The calculated results of the annual outdoor effective dose rates for the soil samples are shown in Table 4.10, and figure 4.7 compares the results for each of the sample.

Table 4.10: Annual Outdoor Effective Dose Rate

Geological formations	Sample ID	Annual Outdoor Effective Dose Rates (mSv/y).
Gneiss-Migmatite	GM1	0.0554± 0.0021
	GM2	0.0455± 0.0022
	GM3	0.0541 ± 0.0030
	GM4	0.0487± 0.0038
Older Metasediments	OM1	0.0304 ± 0.0019
	OM2	0.0386± 0.0021
	OM3	0.0360 ± 0.0011
	OM4	0.0357± 0.0012
Older Granite	OG1	0.0655 ± 0.0038
	OG2	0.0665± 0.0025
	OG3	0.0538 ± 0.0025
	OG4	0.0748± 0.0039
Gundumi/Illo formation	GF1	0.0253 ± 0.0010
	GF2	0.0253± 0.0010
	GF3	0.0208 ± 0.0015
	GF4	0.0232± 0.0059
Taloka formation	TF1	0.0209 ± 0.0012
	TF2	0.0202± 0.0010
	Range	**0.0202± 0.0010 to 0.0748 ± 0.0039**
	Mean	**0.0412± 0.0040**

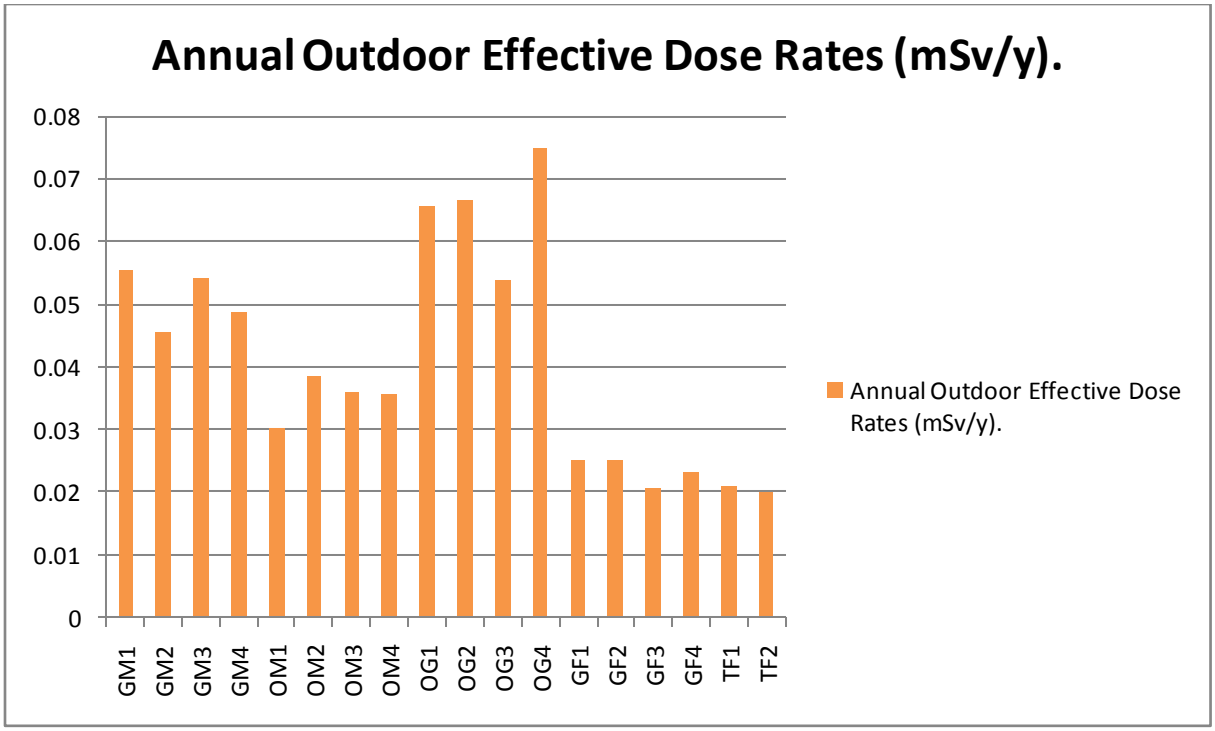


Figure 4.7: Annual Outdoor Effective Dose Rate for each sample.

4.4.6 Excess lifetime cancer risk (ELCR)

Excess Lifetime Cancer Risk (ELCR) in the studied area has been estimated based on the calculated values of annual effective dose (H_R). The ELCR for the outdoor exposure due to TGRD is 137.6×10^{-6} and ranged from $(71.0 \pm 4.0) \times 10^{-6}$ to $(262.0 \pm 14.0) \times 10^{-6}$, with a mean value of $(144.0 \pm 14.0) \times 10^{-6}$ from the spectrometric measurement. The mean ELCR values obtained in this study are less than the world average value 1160.0×10^{-6} (Isinkaye and Emelue, 2015). Table 4.11 shows the calculated values of ELCR obtained, while figure 4.8 compares the results of each sample.

Table 4.11: Excess Lifetime Cancer Risk

Geological formations	Sample ID	ELCR ($\times 10^{-6}$)
Gneiss-Migmatite	GM1	194.0 ± 7.0
	GM2	159.0± 8.0
	GM3	189.0 ± 11.0
	GM4	170.0± 13.0
Old Metasediments	OM1	106.0 ± 7.0
	OM2	135.0± 7.0
	OM3	126.0 ± 4.0
	OM4	126.0± 4.0
Older Granite	OG1	229.0 ± 13.0
	OG2	233.0 ± 9.0
	OG3	188.0± 9.0
	OG4	262.0 ± 14.0
Gundumi/Illo formation	GF1	89.0± 4.0
	GF2	89.0 ± 4.0
	GF3	73.0± 5.0
	GF4	81.0 ± 21.0
Taloka formation	TF1	73.0± 4.0
	TF2	71.0 ± 4.0
	Range	**71.0 ±4.0 to 262.0± 14.0**
	Mean	**144.0± 14.0**

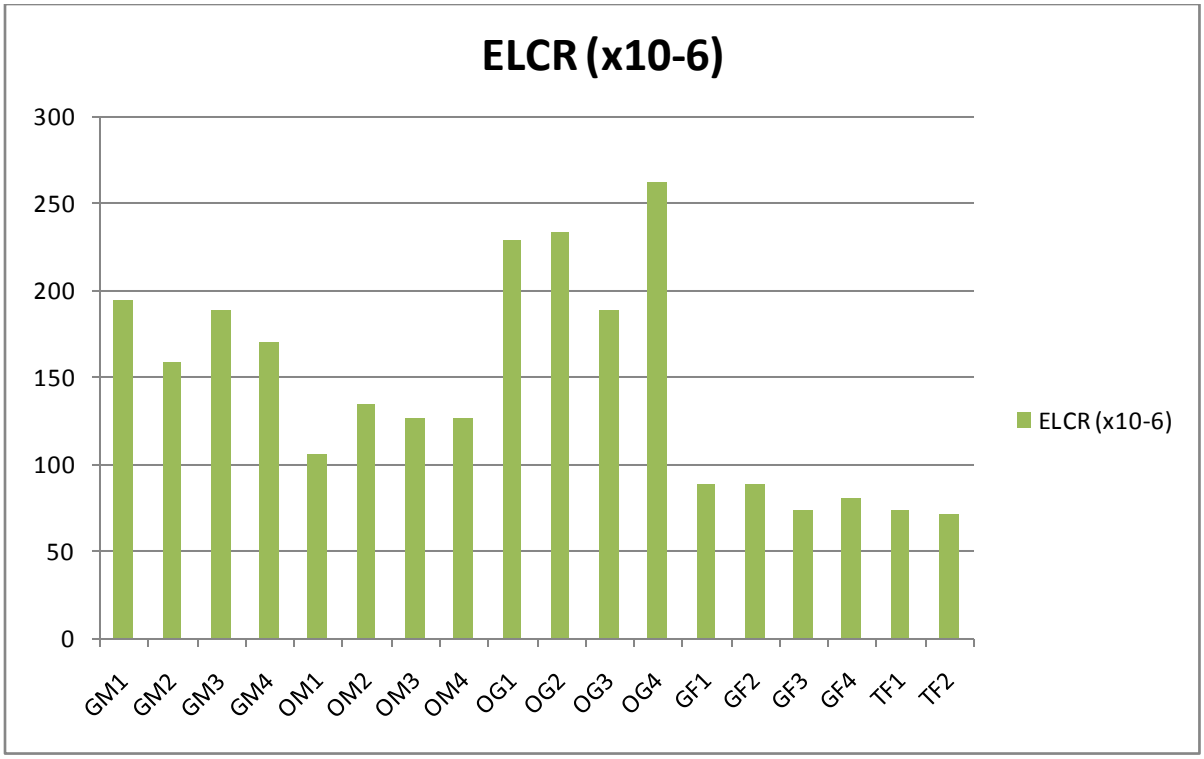


Figure 4.8: Excess Lifetime Cancer Risk for each sample.

CHAPTER FIVE

SUMMARY, CONCLUSION AND RECOMMENDATIONS

5.1 Summary

Environmental radiology is the science study of radiation, detection and protection for human and the environment. Radiation is part of the environment, irrespective of the location on the earth's surface and has been so since the creation of the earth. The radioactive substances are continuously emitting ionizing radiation that affects living organisms due to continuous exposure from the ground, building materials, air, and from human body. The levels of exposure of the terrestrial radionuclides in the soils of any region of the Earth depend mainly on the geological and geographical land formations. There are five geological formations in the study area; Gneiss-Migmatites, Old Metasediments, Older Granite,Guadumi/Illo and Taloka formations. The TGRD rates in air and activity concentrations in the soil were quantified using handheld Inspector Alert Nuclear Monitor and HPGe spectrometer.Older Granite formation recorded the highest values in mean TGRD rates, activity concentrations and radiological health hazard parameters.

5.2 Conclusion

This study has produced baseline data on TGRD, activity concentrations of U-238, Th-232 and K-40 as well as the radiological implications in the air and soil samples of the NorthernZamfara State, Nigeria. These were quantified using Handheld Inspector Alert Nuclear Radiation Monitor and HPGe spectrometer.

The measured TGRD rates ranged from 20.00 to 61.43 nGy/h, with a mean value of 31.99 $\pm$ 0.61 nGy/h. Older Granite formation recorded the highest mean value of TGRD rate (38.90 $\pm$ 2.68 nGy/h). These mean values are less than the world average value of 59 nGy/h.

The radiological map of the studied area was produced using ArcGIS software version 10.3. The map shows some areas of Bakura, Maradun, Birnin-Magaji, Zurmi and KauraNomadalocal governments recorded high TGRD rate. These are the areas dominated by Gneiss-Migmatite and Older Granite.

The mean activity concentrations of U-238, Th-232, and K-40 in the soil samples are 19.43 ± 2.22, 23.26 ± 2.43, and 268.62 ± 39.03 Bq/kg respectively. Moreover, Older Granite formation recorded the highest activity concentrations of U-238, Th-232, and K-40 as 44.22±5.78, 43.96±4.64, and 527.36±12.38 respectively. This could be traced to the fact that Older Granite formation is associated with igneous rocks, which contain high contents of radioactive elements (Bruce, 2009). These results were compared with other studies carried out in other countries and the worldwide average values of activity concentrations for the primordial radionuclides reported by UNSCEAR, 2000 and were found to be less than the world recommended average.

The radiological hazards to the public in the studied area were estimated. The mean values of radium equivalent activity, external hazard index, and activity utilization index for the soil samples were found to be 71.674±7.099 Bq/kg, 0.1936±0.0192, and 0.4688±0.0448 respectively. Moreover, the absorbed gamma dose rates, annual outdoors effective dose rates, and excess lifetime cancer risk were calculated for both TGRD rate measurements and spectrometric analysis of the soil samples. Their mean values were 31.99nGy/h, 0.0393 mSv/y and 137.6 × 10^{-6} respectively for TGRD rates measurements, and 33.467±3.367 nGy/h, 0.0412±0.0040 mSv/y and (144.0±14.0) × 10^{-6} respectively for spectrometric measurement. These calculated radiological parameters were found to be less their world recommended average values of 370 Bq/kg, 1.0, 2.0, 60.0 nGy/h, 0.07 mSv/y and 1160 × 10^{-6} respectively.

Finally, the data obtained in this study can serve as a baseline data which could be used in formulating safety standards of national guidelines for Nigeria in line with international recommendation.

5.3 Recommendations

Based on this study, the following recommendations were made:

1. Similar research should also be carried out at the Southern part of the State.
2. Determination of gross alpha and beta activity concentrations in drinking water sources in the studied area should be carryout.
3. Assessment of radiological concentrations in the foodstuff grown in the studied area should be carryout.

REFERRENCES

Augustine, K. A., and Aku, M. O. (2013). Gamma Radiation Measurements and Dose rates in Cement used in Nigeria. Nigerian Journal Physics. 24: 91-95

Avwiri, G. O., Osimobi, J. C., and Agbalagba, E. O. (2012).Evaluation of Radiation Hazard Indices and Excess Lifetime Cancer Risk Due to Natural Radioactivity in Soil profile of Udi and Ezeagu Local Government Areas of Enugu State, Nigeria. 3 Comprehensive Journal Earth Environmental Science 1(1): 1- 10.

Avwiri, G. O., Osimobi, J. C., and Agbalagba, E. O. (2014). Estimation of Radiation Hazard Indices and Excess Lifetime Cancer Risk associated with river water, Soil and sediments from Mini-Okoro/Oginigba Creek, Port Harcourt, River State, Nigeria. Comprehensive Journal Earth Environmental Science 3(1): 53- 63.

Aznan, F. I., Muhamad, S. Y., Amran, A. M., Ismail, B., Redzuwan, Y. and Irman, A. R. (2009). Radiological Studies of Naturally Occurring Radioactive Materials in some Malaysian's Sand used in Building Construction. The Malaysian Journal of Analytical Sciences. 13(1): 29-35

Bruce, W. H. (2009). Natural Radioactivity in the Geologic Environment.National Nuclear Security Administration Nevada Site Office CEMP. July 28, 2017.

Christian, N. (2014). What are the Effects of Radiation on Humans? What is Radiation Poisoning? Retrieved from www.medicalnewstoday.com/articles/219615.php on August 10, 2017

Evwaraye, A. O., Mgbenu, E. N., and Okeke, P. N. (2006).Electromagnetism and Modern Physics.Nigerian University Physics Series. ISBN 10: 978-029-252-7, 13: 978-978-029-252-2.

Faanu, A., Darko, E., and Ephraim, J. (2012).Determination of Natural Radioactivity and Hazard in Soil and Rock samples in a Mining Area in Ghana, West Africa. Journal of Applied Ecology 19(1): 34-36

Gabdo, H. T., Ramli, A. T., Saleh, M. A., Sanusi, M. S., Garba, N. N. and Aliyu, A. S. (2014). Radiological Hazard Associated with Natural Radionuclide Concentrations in the Northern part of Pahang State, Malaysia. Environ Earth Sci. 73: 6271-6281. doi 10.1007/s12665-014-3850-0

Garba, N. N., Ramli, A. T., Saleh, M. A., Sanusi, M. S., and Gabdo, H. T. (2014).Terrestrial Gamma Radiation Dose Rates and Radiological Mapping of Terengganu State, Malasysia.Journal of Radioanalytical and Nuclearm Chemistry. 303(3):1785 – 1792. doi:10.1007/s10967-014-3818-2

Garba, N. N., Ramli, A. T., Saleh, M. A., Sanusi, M. S., and Gabdo, H. T. (2015).Terrestrial Gamma Radiation Dose Rates and Radiological Mapping of Terengganu State, Malasysia.Journal of Radioanalytical and Nuclearm Chemistry. 303(3):1785 – 1792. doi:10.1007/s10967-014-3818-2

Garba, N. N., Ramli, A. T., Saleh, M. A., Sanusi, S. M., and Gabdo, H. T. (2016a).Radiological Mapping of Kelantan, Malaysia, Using Terrestrial Radiation Dose

Rate. Isotope Environ Health Studies. 52(3):214-218. doi:10.1080/10256016.2016.1095189

Garba, N. N., Ramli, A. T., Saleh, M. A., Sanusi, M. S., Gabdo H.T., and Aliyu A. S., (2016b). The Potential Health Hazards of Chronic Exposure to Low - dose Natural Radioactivity in Terengganu, Malaysia. doi 10.1007/s12665-015-5217-6. Springer – Verlag Berlin Heidelberg 2016

Girigisu, S., Ibeanu, I. G. E., Adeyemo, D. J., Onoja, R. A., Bappah, I., and Okoh, S. (2013). Assessments of Radiological Levels in Soils from Bagega Artisanal Gold Mining exercises at Bagega, Zamfara State, Nigeria. Arch Applied Science Research, 2013

Hossain, I., Sharip, N., and Viswanathan, K. K. (2012).Efficiency and Resolution of HPGe and NaI(Tl) Detectors using gamma-ray Spectroscopy. Scientific Research and Essays. 7(1): 86 – 89. ISSN:1992-2248. doi:10.5897/SRE11.1717

Ibrahim, G. G., Nasiru, R., and Viva, Y. I. (2015). Assessment of Radiation Exposure Levels due to Naturally Occurring Radionuclides in Tin Mining/Processing Sites around Toro Bauchi State, Nigeria.

ICRP (2008).Radiation Dose to Patients from Radiopharmaceuticals.Addendum 3 to ICRP publication 53.ICRP Publication 106. Ann. ICRP 38 : 1-2.

Innocent, A. J., John, O., Ali, H., Onimisi, M. Y., Jonah, S. A., and Nwodo, N. A. (2014). Radiological Safety Assessment of some Mine sites at Gusau and Environs, Nigeria. Advancement in Scientific and Engineering Research 2(2):23-28. ISBN 2384-7336 Research Paper. Science Web Publishing

International Medcom, Inc (IMI) (2015). Inspector Alert^{TM} Nuclear Radiation Monitor Operating Manual. Copyright (1996, 2005, 2013, 2015) by International Medcom, inc

Isinkaye, M. O. and Emelue, H. U. (2015).Natural Radiactivity Measurements and Evaluation of radiological Hazards in Sediment of Oguta Lake, South East Nigeria. Journal of Radiation Research and Apllied Sci. 8: 459-469. doi.org/10.1016/j.jrras.2015.05.001

Khandaker, M. U. (2011). High Purity Germanium Detector in Gamma Ray Spectrometry.International Journal of Fundamental Physical Sciences. ISSN: 2231-8186. 1(2): 42- 46. Retrieved from http://fundamentaljournals.org/ijfpss

Laurie, B. (2018). How do Landforms Affect Human?Retrieved from https://sciencing.com/do-landforms-affect-humans-8611414.htmlon May 22, 2018.

Lee, S. K., Wagiran, H., Ramli, A. T., Apriantoro, N. H., and Wood, A. K. (2009). Radiological Monitoring: Terrestrial Natural Radionuclides in Kinta District, Perak, Malaysia. Journal Environmental Radioactivity 100(5):368-374

Mirion Technologies, Inc (MTI) (2016). Standard Electrode Coaxial Ge (SEGe) Detectors.Copyright 2016 Mirion Technologies (Canberra), Inc.

Nabil, M. H., Nassif, A. M., Mohamed, F. H., and Ebrahim, S. (2015). Assessment of Natural radioactivity in Fertilizers and Phosphate Ore Egypt. Journal of Taibah University for Science 10: 296-306. http://dx.doi.org/10.1016/j.jtusci.08.009

Najib, M. U., Jona, S. A. andMusa, J. A. (2015). Radiological Assessment of Water and Sediments of Zobe Dam Dutsinma in Katsina State for Natural Radionuclides

National Council on Radiation Protection (NCRP) and Measurements (2009). Ionizing Radiation Exposure of the Population of the United States, Bethesda, Md. ISBN: 978-0-929600-98-7. NCRP No. 160.

N.G.S.A., (2013).Geological and Mineral Map of Zamfara State, Federal Republic of Nigeria. National Geo-Sciences Research and Labouratories Centre (N.G.R.L.C), Cartographic section Kaduna Office.

Nuhu, G. O. (2009). Geology and Mineral Resources of Nigeria.Springer Dordrecht Heidelberg London New York. ISBN: 978-3-540-92684-9. doi 10.1007/978-3-540-92685-6

Olusegun, A. T., Adeyemo, D. J. and Sadiq, U. (2014). Assessment of Naturally Occurring Radioactive Materials from a Superphosphate Fertilizer Company in Kaduna, Nigeria using High Purity Germanium Detector.

Osimobi, J. C., Agbalagba, E. O., Avwiri, G. O., and Ononugbo, C. P. (2015). GIS Mapping and Background Ionizing Radiation (BIR) Assessment of Solid Mineral Mining Sites In Enugu State, Nigeria. Open Access Library Journal, 2: e1979. http://dx.doi.org/10.4236/oalib.1101979

Patil, S. S., Patra, R. P., Murali, S., Singh, R., Pradeepkumar, K. S., Vidya, S. D., and Patra, P. (2015). Radiological Mapping of Bhubaneswar City.INIS Environmental Sciences (S54).INIS 46(33).

Ragbu, Y., Ravisankar, R., Chandrasekaran, A., Vijayagopal, P. and Venkataraman, B. (2015). Assessment of Natural Radioactivity and Radiological Hazard in Building Materials used in the Tiruvannamalai District, Tamiluadu, India, using a Statistical Approach. Journal Taibah University of Science. doi.org/10.1016/j.jtusci.2015.08.004

Ramli, A. T., Apriantoro, N. H., Wagairan, H., Wood, A. K., and Kuan, L. S.(2009). Health Risk Implications of High Background Radiation Dose rate in Kampung Sungai Durian, Kinta District, Perak, Malaysia. Global Journal Health Science 1(2): 140

ResearchGate:https://www.researchgate.net/profile/Change_Tan/publication/313744940/figure/fig4/AS:462661361733633@1487175421068/fig-5-Decay-Series-of-A-Uranium-238-238-U-B-uranium-235-235-U-and-C.png

Saleh, M. A., Ramli, A. T., Alajerami, Y., and Aliyu, A. S. (2013). Assessment of Environmental 226Ra, 232Th and 40K Concentrations in the region of elevated radiation background in Segamat District, Johor, Malaysia. Journal Environmental Radioactivity. 124: 130-140

Shahbazi G. D. (2003). Natural Background Radiation Dosimetry in the highest Altitude Region of Iran. Journal Radiation Research. 44: 285 – 287 (Publication Media).

Shahbazi, G. D., Mahrdad, G., and Samaneh, S. (2013). A Review on Natural Background Radiation. Retrieved from doi:10.4103/2277-9175.115821

Sharma, P., Kumar, M. P., and Mishra, K. P. (2014).Terrestrial Gamma Radiation Dose Measurement and Health Hazard along River Alaknanda and Ganges in India.Journal of Radiation Research and Applied Sciences.doi.org/10.1016/j.jrras.2014.09.011

Sidell, A. (2002). Natural and Artificial Radioactivity.Retrieved from http://www.chm.bris.ac.uk/webprojects2002/sidell/NAT&ART.htmon 30th August, 2017.

Tufail, M. (2012).Environmental Monitoring and Assessment.184: 5663 – 5667.doi:10.1007/s10661-011-2370-6

Tzortzis, M., Tsertos, H., Christofides, S., and Christodoulides, G., (2002). Gamma-ray Measurements of Naturally Occurring Radioactive Samples from Cyprus Characteristic Geological Rocks.

Tzortzis M., Svoukis E., and Tsertos H. (2004).A Comprehensive Study of Natural Gamma Radioactivity Level and Associated Dose rates from Surface Foils in Cyprus.Radiation Protection Dosimetry. 109: 17 – 24 (Publication Media).

Udoka, O. (2010). The Lead Poisoning Crisis in Zamfara State, Nigeria. Nigerian Correspondent, Africa Cradle. Retrieved from (www.afriaccradle.com/the-lead-poisoning-crisis-in-zamfara-state-nigeria) on 10th July, 2017.

United Nations Scientific Committee of the Effect of Atomic Radiation (UNSCEAR) (2000).Sources and Effects of Ionizing Radiation. Annex B: Exposure from Natural Radiation, Report on General Assembly; New York City: USA. 1: 84 – 156, ISBN: 90-441-1195-7

Webmaster (2000).Detectors.Retrieved from www2.lbl.gov/abc/wallchart/chapters/12/2.html Retrieved on 6th August, 2016.

Wikimedia Commons.https://commons.m.wikimedia.org/wiki/file:potassium-40-decay-schremme.svg

World Nuclear Association (WNA) (2016) Report. Retrieved from www.world-nuclear.org/information-liberary/safety-and-security/radiation-and-health/naturally-occurring-radioactive-materials-norm.aspx

Zeb, J., Wasim, M., Rashid, A., and Arshed, W. (2015).Radiological Mapping of the Area around Two Research Reactors in Islamabad.Journal of Radioanalytical and Nuclear Chemistry. 306(2): 451 – 455. doi:10.1007/s10967-015-4200-8

APPENDIX I: Measured TGRD rates with the coordinates

S/N	FORMATIONS	Dose Rate (nGy/h)	Latitude (N)	Longitude (E)
1	Taloka formation	28.57140	$12^0$57′43.0″	$006^0$29′21.1″
2		21.42855	$12^0$57′10.9″	$006^0$37′10.1″
3		34.28568	$13^0$03′53.1″	$006^0$29′00.0″
4		29.99997	$13^0$01′42.7″	$006^0$30′08.9″
5		28.57140	$13^0$04′17.4″	$006^0$30′32.5″
6		22.85712	$12^0$52′46.9″	$006^0$40′46.2″
7		22.85712	$12^0$40′37.2″	$006^0$17′31.9″
8		25.71426	$12^0$40′05.1″	$006^0$17′33.8″
9		24.28569	$12^0$39′18.0″	$006^0$07′49.8″
10		29.99997	$12^0$34′41.0″	$005^0$59′43.1″
11		37.14282	$12^0$30′04.1″	$006^0$10′08.2″
12		29.99997	$13^0$08′12.6″	$006^0$18′57.9″
13		28.57140	$13^0$04′47.0″	$006^0$18′57.9″
14		32.85711	$13^0$01′47.1″	$006^0$07′37.0″
15		35.71425	$12^0$57′10.9″	$006^0$04′04.9″
16		24.28569	$13^0$06′09.8″	$006^0$25′50.1″
17		25.71426	$12^0$37′57.0″	$005^0$44′22.8″
18		27.14283	$12^0$39′52.7″	$005^0$45′39.9″
19		42.85710	$12^0$42′33.3″	$005^0$43′57.1″
20		37.14282	$12^0$44′45.1″	$005^0$51′30.9″
21		29.99997	$12^0$37′12.1″	$005^0$39′00.3″
22		39.99996	$12^0$30′08.0″	$005^0$33′58.3″
1	Gundumi-Illo formation	32.85711	$13^0$03′44.8″	$006^0$34′35.9″
2		24.28569	$12^0$50′19.7″	$006^0$02′54.3″

3	32.85711	$13^0 02' 57.8''$	$006^0 37' 55.1''$
4	29.99997	$13^0 01' 15.0''$	$006^0 35' 14.5''$
5	24.28569	$12^0 59' 25.8''$	$006^0 39' 44.3''$
6	25.71426	$12^0 57' 36.6''$	$006^0 44' 07.7''$
7	29.99997	$13^0 00' 17.2''$	$006^0 49' 54.6''$
8	31.42854	$13^0 04' 08.5''$	$006^0 49' 35.4''$
9	24.28569	$13^0 07' 34.1''$	$006^0 42' 24.9''$
10	28.57140	$12^0 52' 32.6''$	$006^0 36' 48.3''$
11	31.42854	$12^0 52' 01.5''$	$006^0 32' 21.4''$
12	35.71425	$12^0 49' 10.0''$	$006^0 31' 23.3''$
13	34.28568	$12^0 48' 48.2''$	$006^0 31' 28.5''$
14	32.85711	$13^0 04' 42.7''$	$006^0 25' 50.4''$
15	35.71425	$13^0 03' 17.1''$	$006^0 23' 53.5''$
16	32.85711	$13^0 02' 47.2''$	$006^0 24' 58.1''$
17	27.14283	$13^0 02' 18.8''$	$006^0 26' 05.4''$
18	29.99997	$12^0 42' 59.3''$	$005^0 52' 25.7''$
19	25.71426	$12^0 40' 46.4''$	$005^0 51' 58.0''$
20	24.28569	$12^0 41' 45.9''$	$005^0 51' 48.0''$
21	28.57140	$12^0 39' 07.7''$	$005^0 49' 44.0''$
22	22.85712	$12^0 33' 46.5''$	$005^0 47' 54.8''$
23	44.28567	$12^0 23' 29.7''$	$005^0 37' 36.8''$
24	29.99997	$12^0 43' 40.3''$	$005^0 52' 30.8''$
25	28.57140	$12^0 54' 01.4''$	$006^0 27' 38.7''$
26	19.99998	$12^0 54' 30.3''$	$006^0 27' 51.2''$
27	25.71426	$12^0 58' 40.8''$	$006^0 22' 49.2''$

28	25.71426	$12^0 54' 56.0''$	$006^0 22' 23.5''$
29	24.28569	$12^0 50' 51.8''$	$006^0 22' 23.5''$
30	22.85712	$12^0 46' 34.2''$	$006^0 25' 16.5''$
31	21.42855	$12^0 47' 34.7''$	$006^0 24' 37.4''$
32	37.14282	$12^0 46' 12.6''$	$006^0 27' 54.6''$
33	28.57140	$12^0 49' 28.3''$	$006^0 17' 28.0''$
34	27.14283	$12^0 56' 00.2''$	$006^0 14' 28.1''$
35	27.14283	$12^0 44' 07.2''$	$006^0 17' 37.5''$
36	32.85711	$12^0 42' 10.4''$	$006^0 1748.3''$
37	31.42854	$12^0 51' 36.8''$	$006^0 09' 13.3''$
39	25.71426	$12^0 38' 23.4''$	$006^0 16' 39.5''$
40	39.99996	$12^0 35' 48.8''$	$006^0 10' 34.7''$
41	28.57140	$12^0 33' 14.2''$	$006^0 09' 48.1''$
42	49.99995	$12^0 31' 49.3''$	$006^0 11' 42.8''$
43	27.14283	$12^0 33' 53.8''$	$006^0 11' 21.6''$
44	31.42854	$12^0 32' 30.5''$	$006^0 07' 23.1''$
45	34.28568	$12^0 34' 09.8''$	$006^0 05' 53.2''$
46	27.14283	$12^0 33' 57.7''$	$006^0 05' 31.4''$
47	19.99998	$12^0 34' 23.1''$	$006^0 01' 58.6''$
48	22.85712	$12^0 44' 07.1''$	$006^0 06' 13.4''$
49	38.57139	$12^0 43' 05.4''$	$006^0 01' 50.0''$
50	19.99998	$12^0 38' 16.3''$	$006^0 00' 39.3''$
51	21.42855	$12^0 38' 18.3''$	$005^0 52' 59.3''$
52	22.85712	$12^0 36' 05.9''$	$005^0 52' 46.8''$
53	28.57140	$12^0 34' 50.7''$	$005^0 53' 03.2''$

54		27.14283	$12^0$32′23.0″	$005^0$56′15.9″
55		24.28569	$12^0$34′45.6″	$005^0$57′04.5″
56		25.71426	$12^0$29′16.6″	$006^0$01′50.0″
57		22.85712	$12^0$27′53.1″	$005^0$56′15.9″
58		22.85712	$12^0$23′36.2″	$005^0$54′01.0″
59		32.85711	$12^0$26′10.3″	$005^0$48′01.3″
60		31.42854	$12^0$29′48.8″	$005^0$47′29.1″
61		28.57140	$12^0$29′42.3″	$005^0$52′31.1″
62		37.14282	$12^0$52′28.1″	$006^0$36′23.6″
1	Old Meta-sediments	25.71426	$12^0$52′20.3″	$006^0$38′15.0″
2		27.14283	$12^0$37′37.8″	$006^0$00′28.5″
3		28.57140	$13^0$04′27.7″	$006^0$31′08.7″
4		34.28568	$13^0$05′22.5″	$006^0$29′39.4″
5		29.99997	$12^0$53′30.5″	$006^0$41′50.1″
6		28.57140	$12^0$39′39.7″	$006^0$35′12.3″
7		37.14282	$12^0$38′52.7″	$006^0$33′44.2″
8		31.42854	$12^0$37′57.3″	$006^0$34′02.4″
9		28.57140	$12^0$38′03.2″	$006^0$35′05.6″
10		32.85711	$12^0$35′12.6″	$006^0$35′05.6″
11		44.28567	$12^0$32′56.4″	$006^0$34′21.3″
12		42.85710	$12^0$32′30.1″	$006^0$32′57.3″
13		37.14282	$12^0$31′49.4″	$006^0$30′50.7″
14		59.99994	$12^0$31′52.6″	$006^0$29′35.9″
15		45.71424	$12^0$31′07.4″	$006^0$28′51.1″
16		55.71423	$12^0$33′46.9″	$006^0$33′19.4″

17		37.14282	$12^0$34′23.2″	$006^0$34′05.4″
18		34.28568	$12^0$36′20.0″	$006^0$35′10.2″
19		34.28568	$12^0$37′00.9″	$006^0$34′44.4″
20		31.42854	$12^0$35′58.7″	$006^0$15′20.2″
21		28.57140	$12^0$29′26.9″	$006^0$11′21.8″
22		25.71426	$12^0$26′10.3″	$006^0$04′43.5″
23		29.99997	$12^0$17′55.6″	$006^0$08′47.6″
24		21.42855	$12^0$11′19.5″	$006^0$03′02.9″
25		34.28568	$12^0$24′19.0″	$006^0$55′09.3″
26		31.42854	$12^0$26′13.8″	$007^0$04′34.7″
27		32.85711	$12^0$24′58.2″	$007^0$02′21.1″
28		27.14283	$12^0$24′48.0″	$006^0$56′10.9″
29		29.99997	$12^0$30′11.8″	$007^0$01′09.1″
30		29.99997	$12^0$34′03.1″	$007^0$02′10.8″
31		27.14283	$12^0$24′14.2″	$006^0$19′10.8″
32		25.71426	$12^0$30′50.6″	$006^0$08′39.5″
33		28.57140	$12^0$18′21.3″	$005^0$59′56.7″
4		27.14283	$12^0$17′04.3″	$006^0$03′52.1″
1	Older Granite (Pan African)	35.71425	$12^0$36′46.9″	$006^0$51′22.1″
2		24.28569	$12^0$34′32.2″	$006^0$51′31.7″
3		42.85710	$12^0$41′36.2″	$006^0$59′11.8″
4		29.99997	$12^0$35′12.3″	$006^0$50′44.5″
5		29.99997	$12^0$34′54.2″	$006^0$52′19.8″
6		39.99996	$12^0$34′31.5″	$006^0$53′06.3″
7		38.57139	$12^0$33′40.2″	$006^0$50′53.9″

8		34.28568	$12^0$32′57.0″	$006^0$49′15.4″
9		31.42854	$12^0$31′54.6″	$006^0$54′48.7″
10		38.57139	$12^0$47′09.3″	$006^0$50′02.9″
11		32.85711	$12^0$47′17.6″	$006^0$50′41.3″
12		32.85711	$12^0$35′46.0″	$006^0$22′55.7″
13		31.42854	$12^0$31′22.6″	$006^0$23′47.1″
14		28.57140	$12^0$25′42.1″	$006^0$23′14.9″
15		34.28568	$12^0$13′25.8″	$006^0$08′09.1″
16		22.85712	$12^0$11′34.5″	$006^0$06′26.3″
17		22.85712	$12^0$23′42.6″	$005^0$50′54.7″
1	Gneiss-Migmatite	35.71425	$12^0$37′09.5″	$006^0$49′05.3″
2		32.85711	$12^0$37′49.3″	$006^0$50′08.0″
3		22.85712	$12^0$43′41.2″	$006^0$33′54.0″
4		61.42851	$12^0$44′39.3″	$006^0$49′13.6″
5		61.42851	$12^0$42′24.3″	$006^0$44′07.7″
6		44.28567	$12^0$44′34.1″	$006^0$50′15.5″
7		28.57140	$12^0$45′59.3″	$006^0$33′08.6″
8		22.85712	$12^0$44′01.8″	$006^0$42′29.6″
9		29.99997	$12^0$25′26.0″	$006^0$36′19.0″
10		31.42854	$12^0$21′48.0″	$006^0$46′45.5″
11		29.99997	$12^0$22′20.7″	$006^0$45′13.0″
12		41.42853	$12^0$22′37.8″	$006^0$42′33.6″
13		45.71424	$12^0$26′41.0″	$006^0$37′20.1″
14		32.85711	$12^0$28′29.0″	$006^0$33′33.9″
15		34.28568	$12^0$32′35.7″	$006^0$39′59.4″

16	44.28567	$12^0 38' 20.1''$	$006^0 27' 54.6''$
17	44.28567	$12^0 37' 49.3''$	$006^0 40' 20.0''$
18	27.14283	$12^0 35' 03.8''$	$006^0 37' 52.0''$
19	39.99996	$12^0 34' 55.1''$	$006^0 39' 53.2''$
20	34.28568	$12^0 21' 22.4''$	$006^0 51' 07.7''$
21	37.14282	$12^0 33' 36.7''$	$006^0 42' 13.8''$
22	55.71423	$12^0 32' 26.6''$	$006^0 42' 41.7''$
23	35.71425	$12^0 33' 51.1''$	$006^0 44' 06.5''$
24	38.57139	$12^0 34' 35.4''$	$006^0 45' 28.9''$
25	32.85711	$12^0 31' 49.5''$	$006^0 44' 02.7''$
26	32.85711	$12^0 35' 01.8''$	$006^0 47' 15.5''$
27	35.71425	$12^0 35' 37.9''$	$006^0 47' 53.8''$
28	47.14281	$12^0 23' 41.2''$	$006^0 39' 38.8''$
29	34.28568	$12^0 40' 09.4''$	$006^0 18' 06.5''$
30	35.71425	$12^0 34' 29.1''$	$006^0 34' 17.9''$
31	42.85710	$12^0 34' 05.4''$	$006^0 34' 21.3''$
32	35.71425	$12^0 32' 41.1''$	$006^0 47' 50.7''$

Appendix II: Plates



Plate I: Inspector Alert Nuclear Radiation Monitor



Plate II: GPS_{MAP} 78



Plate III: Prepared Soil Samples



Plate IV: HPGe Spectrometric Setup